Chapter 3 Gravity Survey

3-1 Survey Methods

As shown in the flow chart (Fig. 2-3-1), the process of gravity survey is largely grouped into "field survey", "data processing" and "analysis".

3-1-1 Field Survey

(1) Gravity measurements

a. Stations

The gravity survey area is shown in Figure 1-2. Gravity measurement was carried out at 517 stations in an area of about 2,000 km^2. The location of the stations is shown in Figure 2-3-2. The station interval was 1.5 - 2.0 km along the traverse.

b. Instrumentation

Two sets of LaCoste G gravimeters were used for field measurements. This gravimeter was selected considering its extremely good transportability, ease of operation and accuracy of measurements. The specifications of the LaCoste gravimeters used are as follows.

Gravimeter No.	G-178	G-204
Year of manufacture	Feb.,1968	May,1969
Operating range	0～7,344.88 mgal	0～7,261.53 mgal
Accuracy	0.02 mgal	
Size	14 × 15× 20 cm	
Weight	8.6 kg	
Power source	12 V battery	
Manufacturer	LaCoste & Romberg(USA)	

The milligal constant(K) and scale constant(κ) for the range used in this survey are as follows.

Gravimeter No.	Counter reading	Milligal constant	Scale constant
G-178	1800	1884.20	1.04760
	1900	1988.96	1.04770
	2000	2093.73	1.04780
G-204	2100	2198.51	1.04795
	1900	1966.54	1.03621
	2000	2070.16	1.03638
	2100	2173.80	1.03655

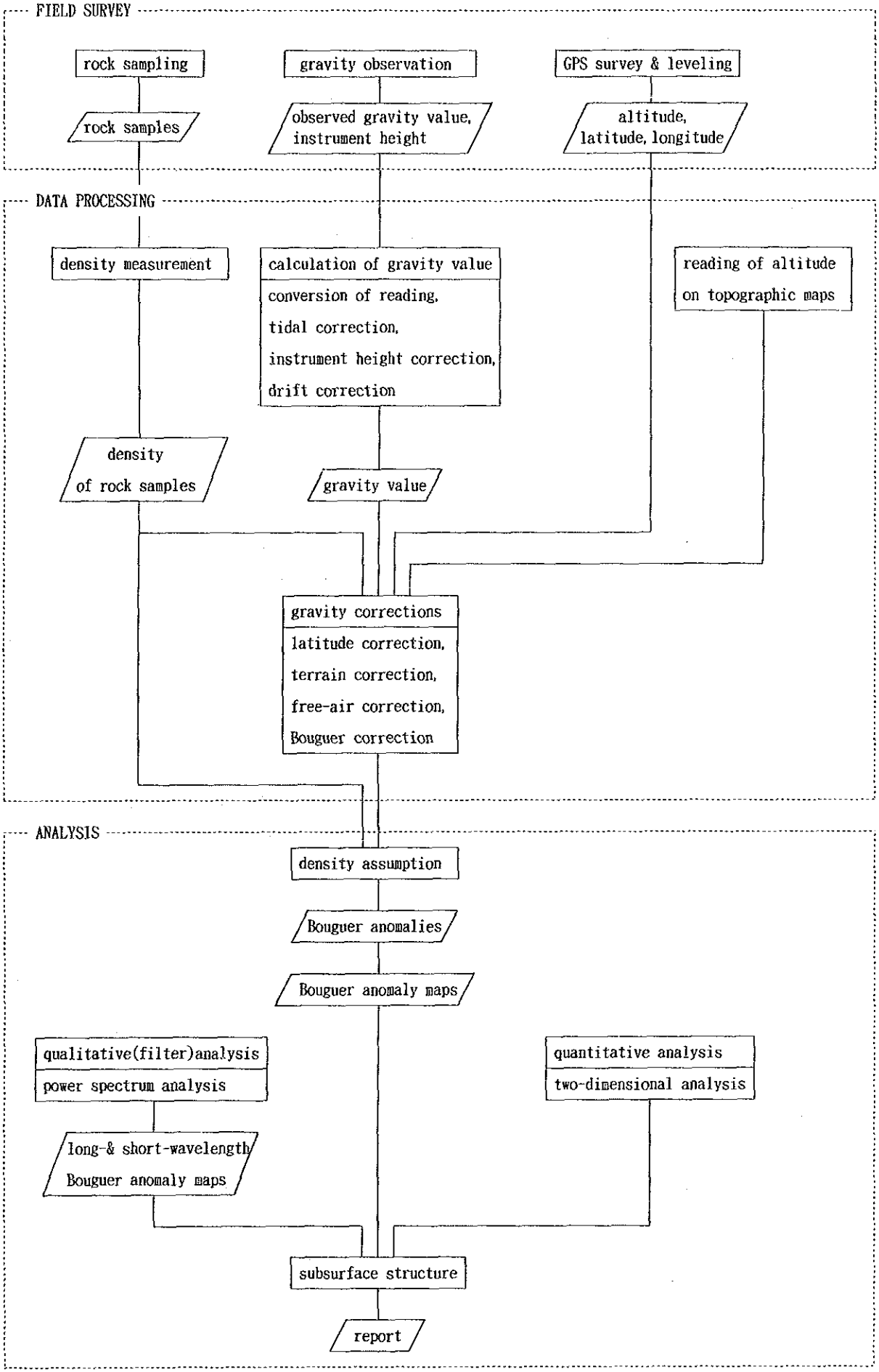

Fig. 2-3-1 Gravity Survey Procedures

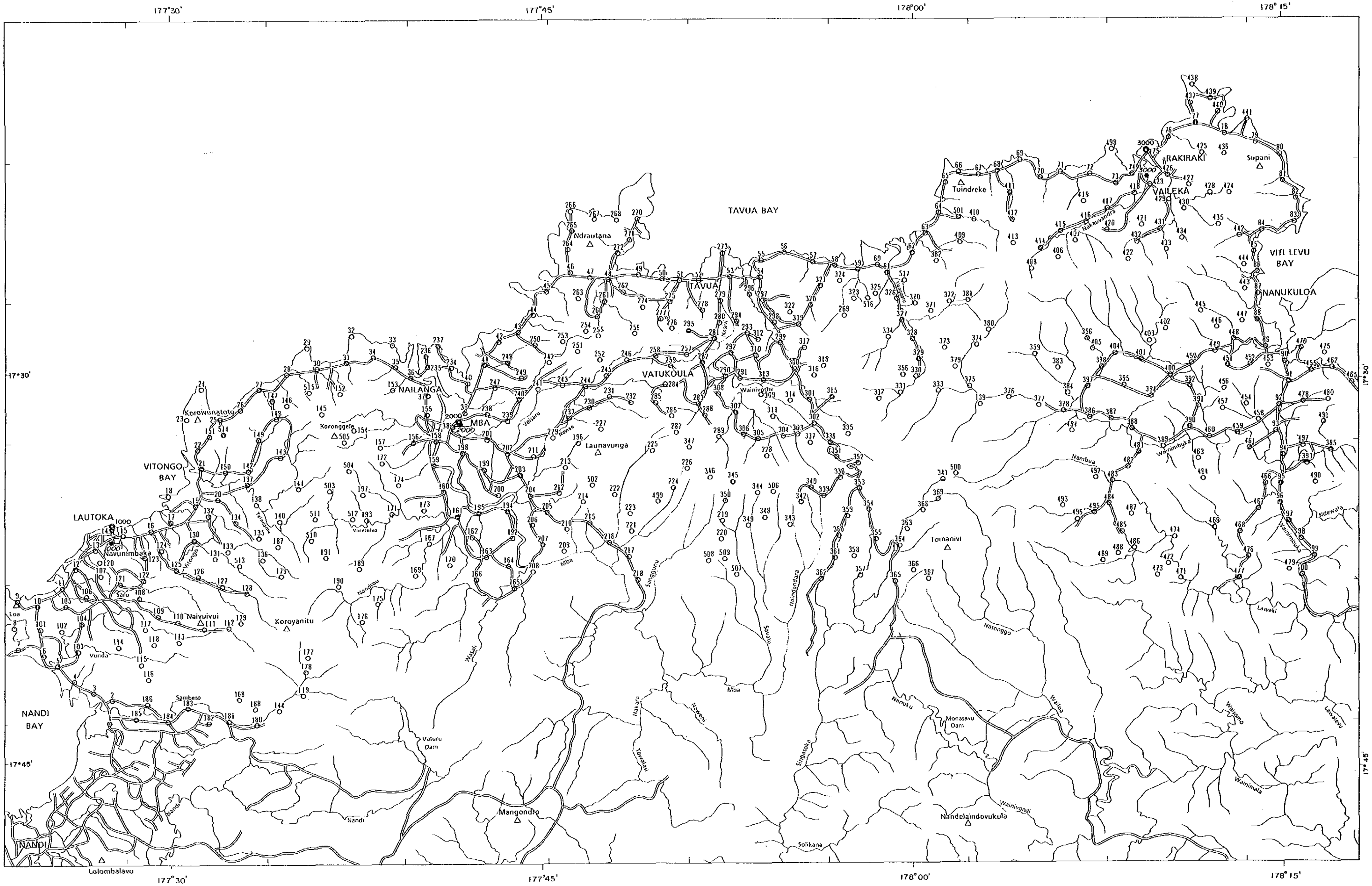

LEGEND

1000 Gravity Base Station

2000 GPS Base Station

123 Station NO.

SCALE 1:250,000

0 5 10 15km

Fig. 2-3-2 Gravity Stations

c. Gravity reference stations and base stations

The gravity values of the gravity reference stations are the standard for determining the gravity values of the base stations. Two reference stations in the Nandi Airport were used for this survey. The gravity values of the two reference stations are as follows (Jezek, P., 1976).

St.No.	Elevation	Latitude	Longitude	Gravity value
189-69	5.0 m	17°45.50'S	177°25.00'E	978,532.11 mgal
189-70	5.0 m	17°47.50'S	177°25.00'E	978,532.11 mgal

The gravity base stations were established at the following three locations.

St.No.	Gravity value	Location
1000	978,537.577 mgal	Front of Sea Breeze Hotel,Lautoka
2000	978,539.868 mgal	Parking lot in front of Mba Hotel,Mba
3000	978,579.704 mgal	Front of room No.106,Rakiraki Hotel,Rakiraki

The locations of the base stations are shown in Figure 2-3-2 by double circles. The detailed maps of the locations and photographs of the stations are shown in Appendix 3. The gravity values of the base stations were determined by base tie from the gravity reference stations.

(2) Leveling and positioning

a. Instrumentation

The instruments used for leveling and positioning of the gravity stations were three sets of 4000ST GPS surveyors (Trimble Navigation Ltd.) and one NA20 automatic level (Wild Heerbrugg Ltd.).

b. GPS survey

The leveling and positioning of the gravity stations were carried out by mainly using the relative positioning of the GPS static survey which is the most accurate method. In this method, the elevation of a station is obtained by measuring the GPS base station and the station simultaneously so that the elevation of each station is calculated relative to that of the GPS base station. Similarly the elevation of the base stations were measured relative to the GPS reference station. For this survey, three base stations were established and their elevation was obtained from the Loa GPS reference station. The elevation of the Loa GPS reference station was obtained by leveling from the Loa Triangulation Station. The elevation, latitude and

longitude of the Loa Triangulation Station, Loa GPS reference station and the base stations are as follows.

St. name	Elevation	Latitude	Longitude	Location
Loa Tri.	33.802 m	17°39'04.4320"S	177°23'37.3909"E	
Loa GPS reference	28.364 m	17°39'03.1"S	177°23'35.6"E	
Base No. 1000	65.531 m	17°36'54.7"S	177°27'15.8"E	On roof of Lautoka Hospital, Lautoka
Base No. 2000	16.083 m	17°32'11.8"S	177°41'22.4"E	On roof of Mba Hotel, Mba
Base No. 3000	12.753 m	17°22'40.0"S	177°09'16.7"E	On roof of Gafoor's Restaurant, Vaileka

The relation of the reference station, GPS base stations and the ordinary stations is as follows.

Loa Triangulation Station → (leveling) Loa GPS reference station → (GPS) Base station No.1000 → (GPS) Stations

→ Base station No.2000 → Stations

→ Base station No.3000 → Stations

The measurement time for each station was 10 - 30 minutes and that for the determination of the elevation of the base station was about one hour.

The latitudes and longitudes were also obtained by GPS measurements. But those by GPS are based on WGS-84 (World Geodetic System) which was anticipated to differ from the system used in Fiji. Therefore, the two systems were compared at several stations where the coordinates are accurately known. The results showed that there are the following descrepancies between the GPS system and the published 1:50,000 topographic map.

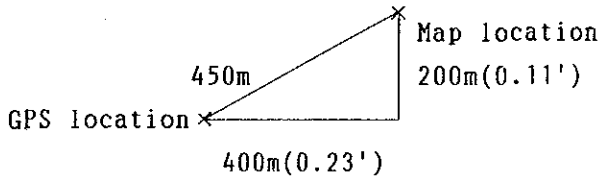

Thus, the coordinates for each station were corrected -0.11'S for latitude and +0.23'E for longitude.

c. Leveling

Conventional leveling was used for stations where the environment was not suitable for GPS measurements and for those with doubtful GPS results. These totaled 42 stations of which the leveling results were used for 25 stations as the final values.

(3) Rock sampling

Rock samples for density measurements were collected from the whole Viti Levu Island considering the stratigraphy and lithology. A total of 38 samples were collected and their locations are shown in Figure 2-2-1.

3-1-2 Data Processing

Data processing for gravity survey largely consists of the following two parts.

① Calculation of gravity values from the dial readings (gravity calculation).

② Calculation of Bouguer anomalies (gravity reduction).

These are processed on the basis of the data files prepared for each station.

(1) Preparation of original data files

The original data file contains; station number, date and time of measurement, gravimeter dial reading, instrument height, latitude, longitude, elevation, terrain correction of "neighbour", code number of gravimeter, leveling method, terrain correction of "close" and other basic data relevant for subsequent processing. These data are stored in a floppy disc.

The format of an original data file is shown in Table 2-3-1.

(2) Calculation of gravity values

In order to calculate the gravity values from the dial readings, "milligal conversion", "tidal correction", "instrument height correction" and "drift correction" are carried out.

a. Milligal conversion

This process converts the dial readings to milligal value. In the case of LaCoste gravimeters, the scale constant slightly changes with the stretching of the spring. Therefore, this conversion is carried out using the milligal constant(K) and scale constant(κ) designated for every 100 units of the

Table 2-3-1 Original Data File Format

Column	Format	Contents		Remarks
1－5	A5	Area name		FIJI
6－7	A2	Sign of base station		ST : base station
8－13	I6	Station No.		
14－15	I2	Year	Observed date	1990→90
16－17	I2	Month		Dec.→12
18－19	I2	Day		5th→05, 15th→15
20－21	I2	Hour		9→09, 15→15
22－23	I2	Minute		6→06, 36→36
24－31	F8・3	Reading value		
32－36	F5・2	Instrument height(m)		
37－44	F8・3	Elevation(m)		
45－52	F8・2	Latitude		South lat. 17°36.91′→ 173691
53－61	F9・2	Longitude		East long. 177°27.26′→1772726
62－66	F5・2	Onshore "neighbour" terrain correction value		$\rho = 2.0$ g／cm^3
67－71	F5・2	Offshore"neighbour" terrain correction value		$\rho = 1.0$ g／cm^3
72－73	I2	Gravimeter No.		Code No. of LaCoste gravimeters 1 : G-150, 2 : G-178, 3 : G-204, 4 : G-206, 5 : G-236, 6 : G-283, 7 : G-286, 8 : G-365, 9 : G-366, 10 : G-579
74	I1	Blank		
75－76	I2	Leveling method		0 : leveling, 6 : GPS
77－80	F4・2	"close" terrain correction value		$\rho = 2.0$ g／cm^3

reading value.

The basic equation for the conversion is as follows.

$$Vr = K + (R - R_0) \times \kappa \qquad (3-1)$$

Vr: Measured value in milligal
R : Gravimeter readings
R_0: Under 100 omitted from R

For example, if R is 2,062.364, R_0 is 2,000, K is 2,093.73, scale constant(κ) is 1.04780. Therefore, the equation will be,

$$Vr = 2,093.73 + (2,062.364 - 2,000) \times 1.04780 \qquad (3-2)$$

b. Tidal correction

The observed gravity values vary periodically within the range of ± 0.2 mgal because of the following two factors. The correction for these variations is the tidal correction.

i) Periodic variation by tidal force.

ii) Very small deformation of the earth by the tidal force (earth tide).

This force is expressed by equation(3-3).

$$U = \frac{3}{2} \cdot G \cdot M \frac{a}{r^3} \{3 (\sin^2 \delta - \frac{1}{3}) \cdot (\sin^2 \phi - \frac{1}{3}) + \sin 2\delta \cdot \sin 2\phi \cdot \cos\theta + \cos^2 \delta \cdot \cos^2 \phi \cdot \cos 2\theta \} \qquad (3-3)$$

U : Tidal force of celestial bodies
G : Gravitational constant
M : Mass of celestial bodies (sun, moon etc.)
a : Distance from the center of the earth to the station (earth's radius)
ϕ : Latitude of the station
r : Distance between the earth and the celestial bodies
δ : Declination of the celestial bodies (angle from the equator)
θ : Hour angle of the celestial bodies (angle between terrestrial and celestial meridian plane)

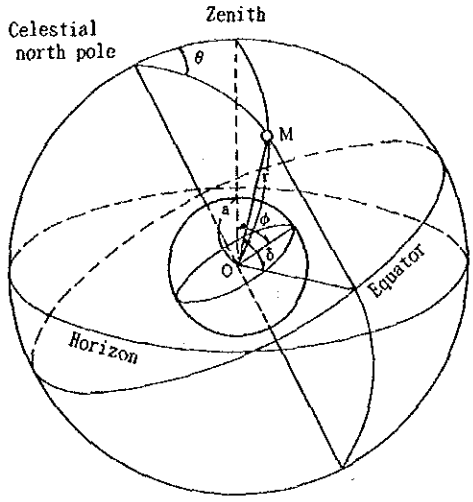

The tidal force of the sun and moon is overwhelmingly greater than that of other celestial bodies. Therefore, the correction for these two bodies will suffice for gravity prospecting.

The gravity variation caused by earth tide has the same sense as that by the tidal force and the rate of change differs somewhat by the elasticity of the rocks of the area, but it is in the order of 20 % of that caused by tidal force. Therefore, in normal tidal correction, the tidal force by the sun and moon is multiplied by 1.20 which is called the tidal constant.

Stationary gravity measurement was carried out from 7.00 o'clock to 24.00 o'clock at 30 minute interval on 26 December 1990 in Suva in order to check the tidal constant for Fiji. The result is shown in Figure 2-3-3 and it is seen that the measured values agree well with the theoretical values of 1.20. Therefore, this value was used during the present survey.

c. Correction for instrument height

This correction is made in order to compensate for the difference of the height for leveling and gravity measurements.

The correction is done by using the vertical normal gravity gradient on the surface of the ellipsoid of revolution - 0.3086 mgal/m - on equation 3-4.

$$Vhi \fallingdotseq \frac{2\gamma_0}{R} hi \fallingdotseq 0.3086\ hi \qquad (3-4)$$

Vhi: Instrument height correction value

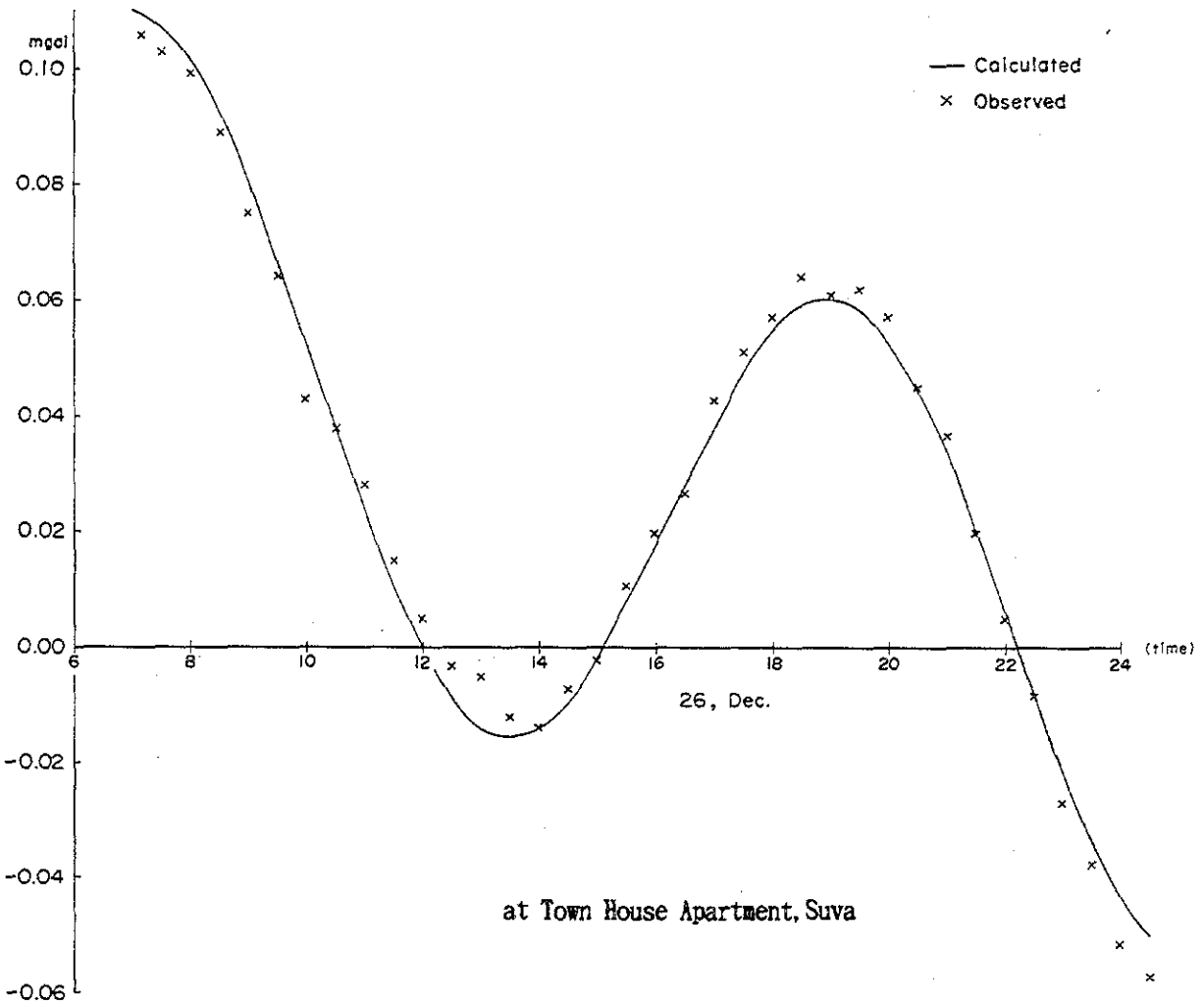

Fig. 2-3-3 Diurnal Gravity Variation

γ_0 : Normal gravity
R : Distance from the earth's center to the station
hi : Height from the leveled point on the earth's surface to the top of the gravimeter

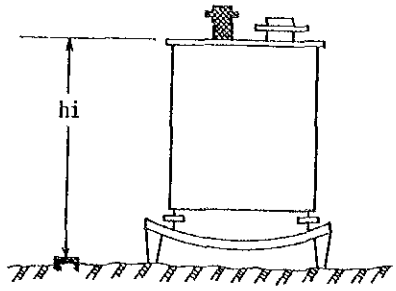

d. Drift correction

The drift is the variation of reading values of the gravimeter caused by the stretching of the spring. The value of the drift is roughly proportional to time. The correction for this drift is done by time-proportional allotment of the closed error for each station. The variation of readings are caused not only by drift, but also by the changes of temperature, atmospheric pressure and mechanical shock during transportation. In practice, these changes are also corrected by this process.

e. Calculation of gravity values

All corrections for measured gravity values (Vr) are expressed by equation 3-5.

$$Vc = Vr + Vt + Vhi + Vd \qquad (3-5)$$

Vc: Corrected gravity value
Vt: Tidal correction value
Vd: Drift correction value

The corrected gravity value Vc shows the relative value of gravity and not the absolute value of gravity. The gravity value of each station is calculated by obtaining the difference of the corrected gravity values between the station and the base station and then adding the gravity value of the base station to this difference. The gravity value of the base station is obtained by separate measurement between the base station and the reference station where the gravity value is known.

(3) Gravity reduction

The process of calculating the Bouguer anomaly values is called the gravity reduction and it consists of "latitude correction", "terrain correction", "atmospheric correction", "free air correction" and "Bouguer correction".

a. Latitude correction

This correction is done by subtracting the standard gravity of the earth from the gravity value. The standard gravity is given as a function of the latitude and normal gravity γ_0 of equation 3-6 is presently used as the standard gravity.

$$\gamma_0 = \frac{a\,\gamma_E \cos^2\phi + b\,\gamma_P \sin^2\phi}{\sqrt{a^2\cos^2\phi + b^2\sin^2\phi}} \qquad (3-6)$$

a: Equatorial radius of the ellipsoid of revolution (6,378.14 km)
b: Polar radius of the ellipsoid of revolution(6,356.75 km)
γ_E: Equatorial normal gravity of the ellipsoid of revolution (978.032 gal)
γ_P: Polar normal gravity of the ellipsoid of revolution (983.218 gal)

However, for practical gravity prospecting, the following approximation is used.

$$\gamma_0 = 978031.85(1 + 0.005278895\,\sin^2\phi + 0.000023462\,\sin^4\phi)\ (\text{mgal}) \qquad (3-7)$$

b. Terrain correction

This correction is made in order to correct the effect of the topographic relief of the vicinity of the stations on gravity values. It is done in a fashion by which high reliefs are shaved off and depressions are buried and a flat surface is assumed. The correction for both cases is positive. The correction for flat surface is 0 mgal and for areas with rugged relief, it may reaches tens of milligals.

For the present survey, the range of terrain correction was set for a radius of 60 km and the area was divided into six correction zones as follows.

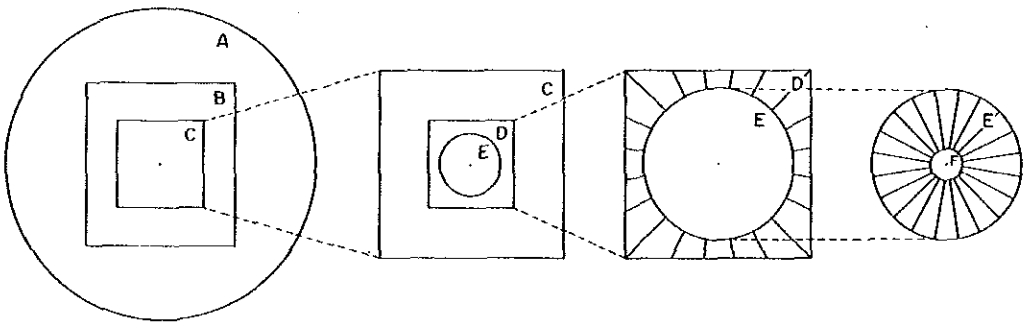

Terrain Correction Concept

Items of Terrain Correction

Zone	Range of correction	Grid interval	Correction type
A	60km radius－zone B	3'(E-W)×2'(N-S)	Far
B	21'(E-W)×16'(N-S)	5"(E-W)×30"(N-S)	Medium
C	5'15"(E-W)×4'(N-S)	1.25"(E-W)×7.5"(N-S)	Near(1)
D	1.25×1.25km－zone E	Pentahedron	Near(2)
E	20m-500m radius from station	Pentahedron	Neighbour
F	20m radium from station		Close

The effect of the terrain is large near the stations and it decreases inversely proportionate to the square of the distance from the station. Therefore, the grid interval is set shorter as it nears the station. The elevation of the grid points is interpolated from the grid elevation data read at constant intervals on the 1:50,000 topographic map. For the elevation of the grid points on A, B and C-E zones, grid data read every 5,1 and 0.25 km intervals from the map were used respectively. For zone F, two dimensional topographic profiles up to 20 m from the station were used for the correction.

c. Atmospheric correction

This is done in order to correct the effect of the atmosphere to gravity measurement. The atmospheric pressure will be integrated to a height of 50 km above the station using the atmospheric density distribution based on standard atmospheric model. The correction value decreases exponentially with altitude. The variation of the correction values, however, can be appproximated by a linear function for altitude below 3 km. And equation 3-8 is usually used for this correction.

$$\delta g_A = 0.87 - 0.0965 \times 10^{-3} H \quad (3-8)$$

δg_A: Atmospheric correction value (mgal)

H : Elevation of the station (m)

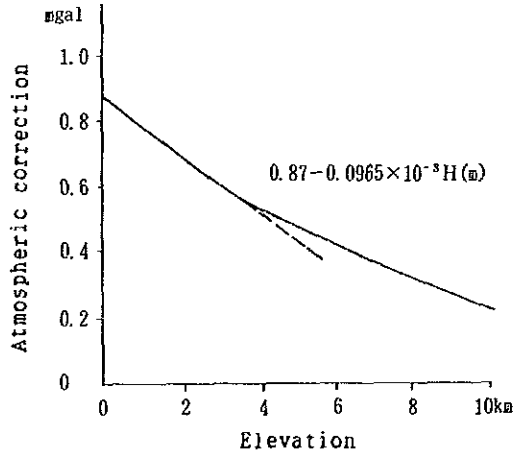

d. Free air correction

The vertical gravity gradient near the earth's surface is -0.3086 mgal/m, and thus the gravity decreases with height. The free air correction corrects the effect of elevation for each station.

$$\delta g_F \fallingdotseq \frac{2\gamma_0 H}{R} \fallingdotseq 0.3086H \qquad (3-9)$$

δg_F : Free air correction value
γ_0 : Normal gravity
R : Distance from the earth's center to the station
H : Elevation from the geoid

The value defined by equation 3-10 is called the free air anomaly.

$$\triangle g_F = g - \gamma_0 + \Sigma \delta g_T + 0.3086H \qquad (3-10)$$

$\triangle g_F$: Free air anomaly
g : Gravity value
$\Sigma \delta g_T$: Terrain correction value

e. Bouguer correction

The difference of the gravity values measured at different elevations corresponds to the attraction of the material (rocks) which exists between the elevations of the stations. Bouguer correction eliminates this difference by setting a datum plane and eliminating material between the datum and a parallel plane passing through each station. Usually geoid is used as the datum. A homogeneous circular slab is assumed to exist between the geoid and a parallel plane including the station for the correction (equation 3-11). The radius of this slab is set at 60 km, the same as the range of terrain correction.

$$\begin{aligned}\delta g_B &= -2\pi G \rho (A + H - \sqrt{A^2 + H^2}) \\ &\fallingdotseq -0.0419\rho (A + H - \sqrt{A^2 + H^2})\end{aligned} \qquad (3-11)$$

δg_B : Bouguer correction value
G : Gravitational constant
ρ : Density, average density of rocks between the geoid and earth's surface
A : Circular slab radius (60 km)
H : Station elevation

f. Bouguer anomaly values

The values obtained by correcting the gravity values for latitude,

terrain, atmosphere, free air and Bouguer are called the Bouguer anomalies and are expressed by equation 3-12.

$$\triangle g_B = g - \gamma_0 + \Sigma \delta g_T + 0.87 - 0.0965 \times 10^{-3} H + 0.3086 H - 0.0419 \rho (A + H - \sqrt{A^2 + H^2}) \quad (3-12)$$

$\triangle g_B$: Bouguer anomaly value

The Bouguer anomaly is defined at the earth's surface and the value varies by the density used for the Bouguer and terrain corrections. Thus the Bouguer anomaly contains information not only on the density structure below the geoid but also the difference of the real and the assumed density used in correction for the rocks between the geoid and the surface.

Tables of relevant data regarding this gravity survey are attached in the Appendices. These data include; location (coordinates and elevation) of stations, gravity values, various correction values, normal gravity values and Bouguer anomalies, and Bouguer anomalies for six different assumed density values.

(4) Preparation of gravity maps

The Bouguer anomaly value of each station was converted to grid point value on rectangular coordinates. This was done in order to draft Bouguer anomaly map using a plotter and to obtain gravity values for filter analysis.

La Porte(1962) method was used for calculating the values for the grid points because the reproducibility of the Bouguer anomaly for each station is very good by this method. The grid interval of 1 km was used and the grid point values were calculated only when more than six stations were included within a range of 10 km radius with over 240 degree angle with the center at the grid point. Three types of isogravity maps (Bouguer anomaly maps) were prepared with correction densities of 2.40, 2.50 and 2.60 g/cm^3.

3-1-3 Analytical methods

(1) Assumption of density

Regarding the most appropriate density correction for a given area, there are largely two methods; density measurement of rock samples and the G-H correlation method.

a. Density measurement of rock samples

i) Method of measurement

The 38 samples collected were weighed in air and in water,and their dry

and wet density was calculated as follows.

$$\text{Natural dry density} \quad \frac{W_1}{W_2 - W_3} \tag{3-13}$$

$$\text{Wet density} \quad \frac{W_2}{W_2 - W_3} \tag{3-14}$$

W_1: Weight in air of samples left in a room (normal temperature) for several days (naturally dried).

W_2: Weight in air of samples immersed in water for 24 hours under natural atmospheric pressure and the surface was wiped with cloth.

W_3: Weight in water after immersion under natural atmospheric pressure for 24 hours.

ii) Measured density

The results of the measurement are laid out in Table 2-3-2. The average wet density for various geologic units is shown in Table 2-3-3. The low average density unit is Verata Sedimentary Group (2.09 g/cm^3) and high average density units are Koroimavua Volcanic Group (2.72), Colo Plutonic Suite (2.78) and Yavuna Volcanic Group (2.68). The average density of all samples is 2.50. The density of Ba Volcanic Group varies greatly from 1.74 to 2.96. There is a large difference of density among various rocks as seen in the right column of Table 2-3-3. Namely, the density of sandstone, siltstone and tuff is under 2.50 and varies significantly, while that of basalt, andesite, breccia, monzonite and diorite is larger than 2.50 with generally small variation. The average densities of various rocks of the survey area are as follows.

Rocks	Number of samples	Average density
sandstone	6	2.19
siltstone	4	2.09
tuff	4	2.06
breccia	5	2.72
basalt,shoshonite	9	2.79
andesite	5	2.61
diorite,monzonite	4	2.74

The density of the rocks of Viti Levu has been measured on many occasions in the past. Some of these data are summarized in Table 2-3-4.

b. G－H correlation

This is a method of calculating the density ρ from the sum of the free

Table 2-3-2 Rock Density

Stratigraphic units	Sample NO.	Rock name	Density (g/cm³)	
			Natural dry	Wet
Verata Sedimentary Group	* C-71	Sandstone	2.21	2.21
	* C-72	Sandstone	2.28	2.29
	* C-73	Sandstone	1.72	1.76
Ba Volcanic Group	C-38	Shoshonite	2.96	2.96
	C-22	Basaltic volcanic breccia	2.76	2.76
	C-23	Basalt	2.83	2.83
	C-6	Basaltic volcanic breccia	2.55	2.55
	C-54	Basaltic volcanic breccia	2.86	2.85
	* C-55	Basaltic tuff	2.18	2.21
	C-56	Basaltic tuff breccia	2.75	2.75
	C-57	Basaltic tuff breccia	2.70	2.71
	C-59	Basalt	2.71	2.72
	C-65	Basalt	2.80	2.80
	BA-102	Shoshonite	2.92	2.92
	BA-103	Sandstone	2.02	2.01
	C-49	Lapilli tuff	2.33	2.37
	C-58	Andesite	2.52	2.53
	AA-91	Monzonite	2.85	2.84
	* C-5	Siltstone	2.17	2.18
	C-2	Micro-diorite	2.54	2.54
	* C-35	Siltstone	1.72	1.74
	* C-64	Siltstone	1.96	1.97
Koroimavua Volcanic Group	C-7	Andesite	2.68	2.68
	C-8	Basalt	2.83	2.82
	WKA-26	Micro-diorite	2.80	2.81
	C-21	Andesite	2.58	2.58
Navosa Sedimentary Group	A-2	Andesite	2.54	2.56
Nadi Sedimentary Group	* C 31	Sandstone	2.38	2.39
Ra Sedimentary Group	* C-62	Andestic tuff	1.61	1.60
Colo Plutonic Suite	WA-130	Diorite	2.78	2.78
Wainimala Group	C-67	Fossil limestone	2.67	2.67
	C-69	Calcareous Siltstone	2.47	2.48
	* C-66	Conglomerate	2.48	2.49
	* C-68	Tuff	2.07	2.07
	A-3	Andesite	2.70	2.70
Yavuna Volcanic Group	G1	Spilite	2.69	2.70
	G3	Trachydolerite	2.66	2.66
	G4	Trachydolerite	2.69	2.69

* : Samples steeped in water for a few minutes

Table 2-3-3 Average Rock Density(Wet)

Age		Stratigraphic units	Number	Average density(g/cm³)			Density(g/cm³) 2.0 2.5
Quaternary	Pleistocene	Verata Sedimentary Group	3	2.09	2.48	2.48	× × ×
Neogene	Miocene to Pliocene	Ba Volcanic Group	19	2.54			+ + + * *
		Koroimavua Volcanic Group	4	2.72	2.49		• •
		Navosa Sedimentary Group	1	2.56			•
		Nadi Sedimentary Group	1	2.39			×
		Ra Sedimentary Group	1	1.60			*
		Colo Plutonic Suite	1	2.78			△
Paleogene	Oligocene	Wainimala Group	5	2.49			* × •
	Eocene	Yavuna Volcanic Group	3	2.68			□□□
Average			38	2.50			

× Sandstone
+ Siltstone
* Tuff
○ Breccia
• Andesite
□ Basalt, Shoshonite
△ Diorite, Monzonite

Table 2-3-4 Average Rock Density from Existing Data

Age		Stratigraphic units	Number	Density (g/cm³)		
Quaternary	Pleistocene	Verata Sedimentary Group	1	2.50	2.54	2.47
Neogene	Miocene to Pliocene	Ba Volcanic Group	46	2.54		
		Navosa Sedimentary Group	1	2.10	2.36	
		Nadi Sedimentary Group	1	2.46		
		Ra Sedimentary Group	3	2.35		
		Medrausucu Group	23	2.37		
		Colo Plutonic Suite	89	2.74		
		Tuva Group	2	2.50		
		Wainimala Group	100	2.69		
Paleogene	Oligocene					
Average			266	2.64		

(compiled a part of data from Rodda P. and Deberal R., 1966)

air gradient and Bouguer gradient ($0.3086-0.0419\rho$) which theoretically equals the gradient of the plots of the stations on a $g-\gamma\phi+\rho T$ (vertical axis) vs elevation H (horizontal axis) diagram. In areas with large and strong gravity anomalies, accurate density values sometimes cannot be obtained by this method.

The G-H correlation chart of this area is shown in Figure 2-3-4. The plots are scattered and the ρ obtained by the least squares method is extremely small at 1.49 g/cm^3.

(2) Methods of gravity analysis

a. Power spectral analysis

This method is used with the objective of separating the long-wavelength anomalies caused by deep-seated structures and the short-wavelength anomalies caused by shallow structures.

The power spectrum P_{mn} is expressed by the equation 3-15, if the relief of the density boundary is irregular when the Bouguer anomalies are expanded by Fourier series.

$$\ln P_{mn}=C-4\pi D\sqrt{\left(\frac{m}{L_1}\right)^2+\left(\frac{n}{L_2}\right)^2} \qquad (3\text{-}15)$$

C : constant

D : Average depth of the density boundary

L_1, L_2 : Lengths of the sides of rectangle

m, n : Wave numbers

When data are plotted with $\ln P_{mn}$ on the ordinate and $\sqrt{(m/L_1)^2+(n/L_2)^2}$ on the abscissa, two or more lines with different gradients can be drawn through these plots. According to the power spectrum theory, each of these lines represents density boundaries at different depths. Lines within low frequency range represent boundaries in deeper zones and those in high frequency range those in shallower zones.

Figure 2-3-5 is a power spectral analysis diagram with assumed density of 2.50 g/cm^3. The grid interval is 1 km for the data used. For the plots in this diagram, three lines, A-C, can be drawn with varying gradients. The following average depth of the density boundary can be calculated from these gradients.

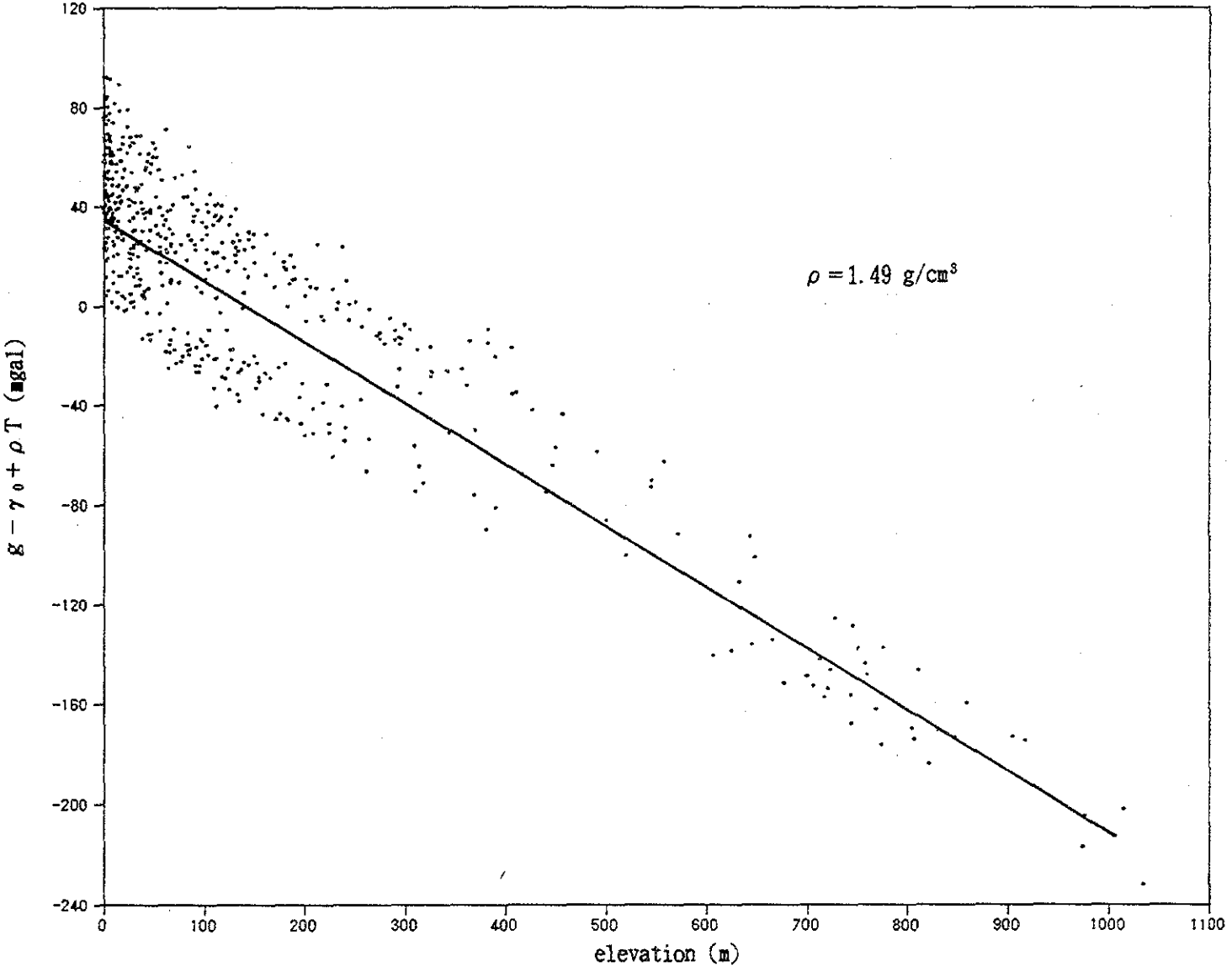

Fig. 2-3-4 Correlation between Gravity and Elevation

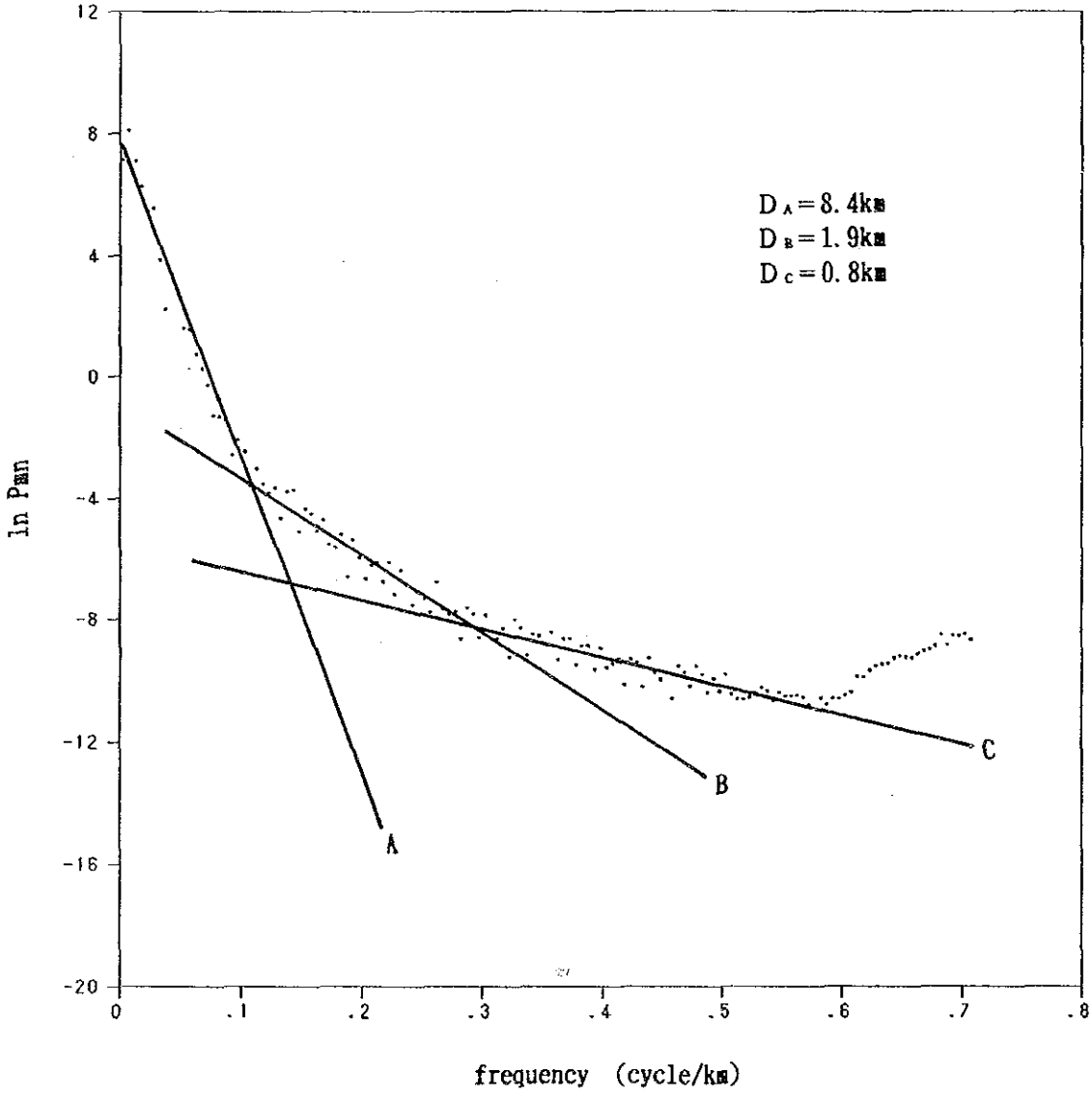

Fig. 2-3-5 Power Spectra of Bouguer Anomalies

A group; average depth D_A=8.4 km
B group; average depth D_B=1.9 km
C group; average depth D_C=0.8 km

From the above, maps were prepared by separating the Bouguer anomalies of this area into those related to the frequency range of Group A and those related to the frequency ranges of Groups B and C. The former is the long-wavelength gravity map and the latter the short-wavelength gravity map.

b. Profile analysis

The profile analysis is a quantitative analysis aimed at constructing a two dimensional model of the subsurface structure which would result in gravity anomalies approximating most closely those measured in the area. The gravity anomalies of the model are calculated by the following Talwani's(1959) equation.

$$g = 2 G \Delta \rho \Sigma Z_i \tag{3-16}$$

$$Z_i = A_i \sin\phi_i - \cos\phi_i \left[\theta_i - \theta_{i+1} + \tan\phi_i \log \frac{\cos\theta_i(\tan\theta_i - \tan\phi_i)}{\cos\theta_{i+1}(\tan\theta_{i+1} - \tan\phi_i)}\right] \tag{3-17}$$

g : Gravity anomaly value
G : Gravitation consttant
$\Delta \rho$: Density contrast(ρ_2-ρ_1)

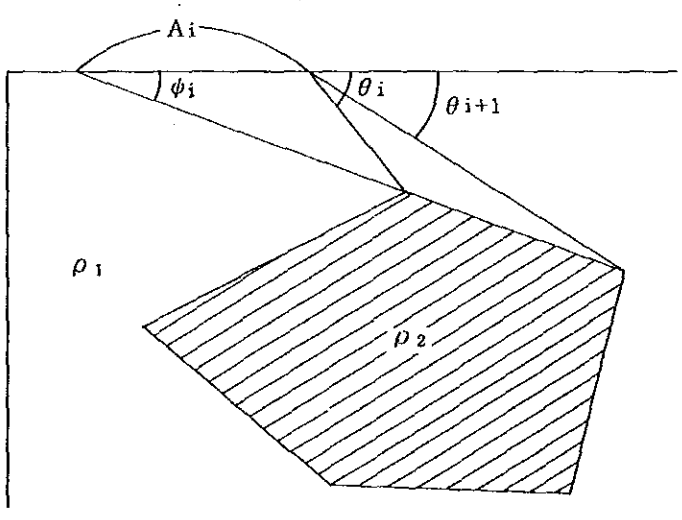

Schematic analysis of two-dimensional density structure by Talwani's method

When the subsurface density structure can be approximated by two-layered model, unique solution can be obtained by; disignating a density contrast and a control depth, and then gradually altering the shape of the density boundary thus approximating the calculated values closer to the measured values. This method is very effective when the subsurface density structure can be approximated by two-layered structure, and good solutions can be obtained in short time.

During this survey, two-layered model analysis was used for the short-wavelength and long-wavelength gravity anomalies.

3-2 Survey Results

3-2-1 Assumption of Density

As mentioned above, density cannot be calculated with tolerable degree of accuracy by the G-H correlation method. The density measurements of rock samples indicated 2.06 to 2.19 g/cm^3 for sedimentary rocks and 2.61 to 2.79 g/cm^3 for igneous rocks. The surface of the gravity survey area is largely covered by igneous rocks and the best correction density would be 2.60 to 2.70. However, it is inferred that sedimentary formations are widely distributed below the igneous units. Therefore assuming that the measured samples represent the total area, the average density of all collected samples, 2.50, was used as the corrected density of the total gravity survey area.

Three types of Bouguer anomaly maps with different corrected densities, 2.40, 2.50 and 2.60 were prepared(Figs.2-3-6 to 8). It is seen from these maps that the shape of the contours are almost the same for the three density values. Therefore, the Bouguer anomaly map with corrected density of 2.50 was used for the analysis.

3-2-2 Bouguer anomaly map

A Bouguer anomaly map with corrected density of ρ=2.50 is shown in Figure 2-3-7. The contour interval is 2 mgal. The Bouguer anomaly values range between -15 mgal to 95 mgal. The contour intervals at the south of Tavua and Rakiraki are very dense. These areas have very high gravity gradient of 7 to 10 mgal/km.

Large scale gravity highs in excess of 50 mgal were found in four localities, west of Ba, Tavua, Rakiraki and east of Nandi. The anomalies of

Tavua, Rakiraki and east of Nandi occur along a ENE-WSW line at similar intervals.

The high west of Ba is oval-shaped and is elongated in the ENE-WSW direction and it has two peaks near the center. The gravity contours under 50 mgal at Tavua have more or less circular shape, while those over 50 mgal are semi-circular with depressed southern side. The high at Rakiraki is oval-shaped elongated in the ENE-WSW direction. It has two peaks which exceed 90 mgal in gravity value. Although the shape of the high east of Nandi is not clear because of the location in the southernmost edge of the gravity survey area, it is inferred to be elongated in the N-S direction. There is a small high protruding eastward from the center of the high east of Nandi.

These gravity highs are characteristically circular to oval in shape and from the scale and the geologic environment, they are considered to reflect the deeper geologic structure of the area.

Gravity low of less than 0 mgal occurs widely from the southern margin of the central part of the gravity survey area to the south of Nanukuloa in the east. Although the shape of this low is not clear because of its occurrence in the southern end of the area, it probably extends in the E-W direction judging from the shape of the contours.

This gravity low is considered to be caused by deep geologic structure, but it also is believed to reflect the shallow structure from the geologic considerations as follows. The low density sedimentary formations which are widely distributed on the surface south of Nanukuloa are most probably the source of the low anomaly in this zone. On the other hand, although high density volcanics cover the surface at the southernmost margin of the central part of the gravity survey area, the low density units developed below the volcanics are reflected in the low anomalies.

3-2-3 Long-wavelength gravity map and short-wavelength gravity map

The long-wavelength and short-wavelength anomalies were separated for Bouguer anomalies of correction density of 2.50 g/cm^3 referring to the results of power spectral analysis.

(1) Long-wavelength gravity map

A Long-wavelength gravity map with 2 mgal contour interval is shown in

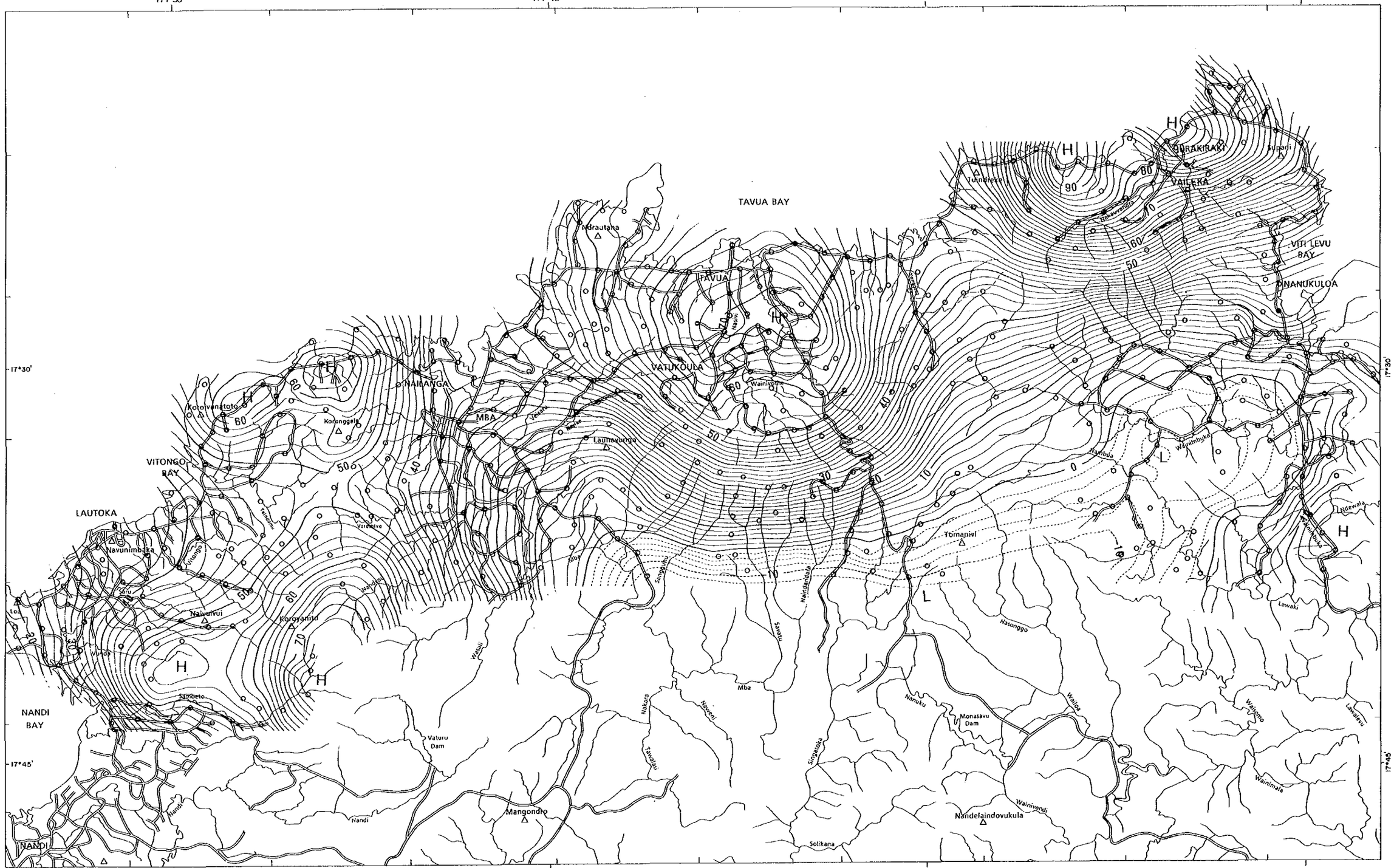

LEGEND

Contour interval : 2 mgal

Fig. 2-3-6 Bouguer Anomaly Map
($\rho = 2.4\ g/cm^3$)

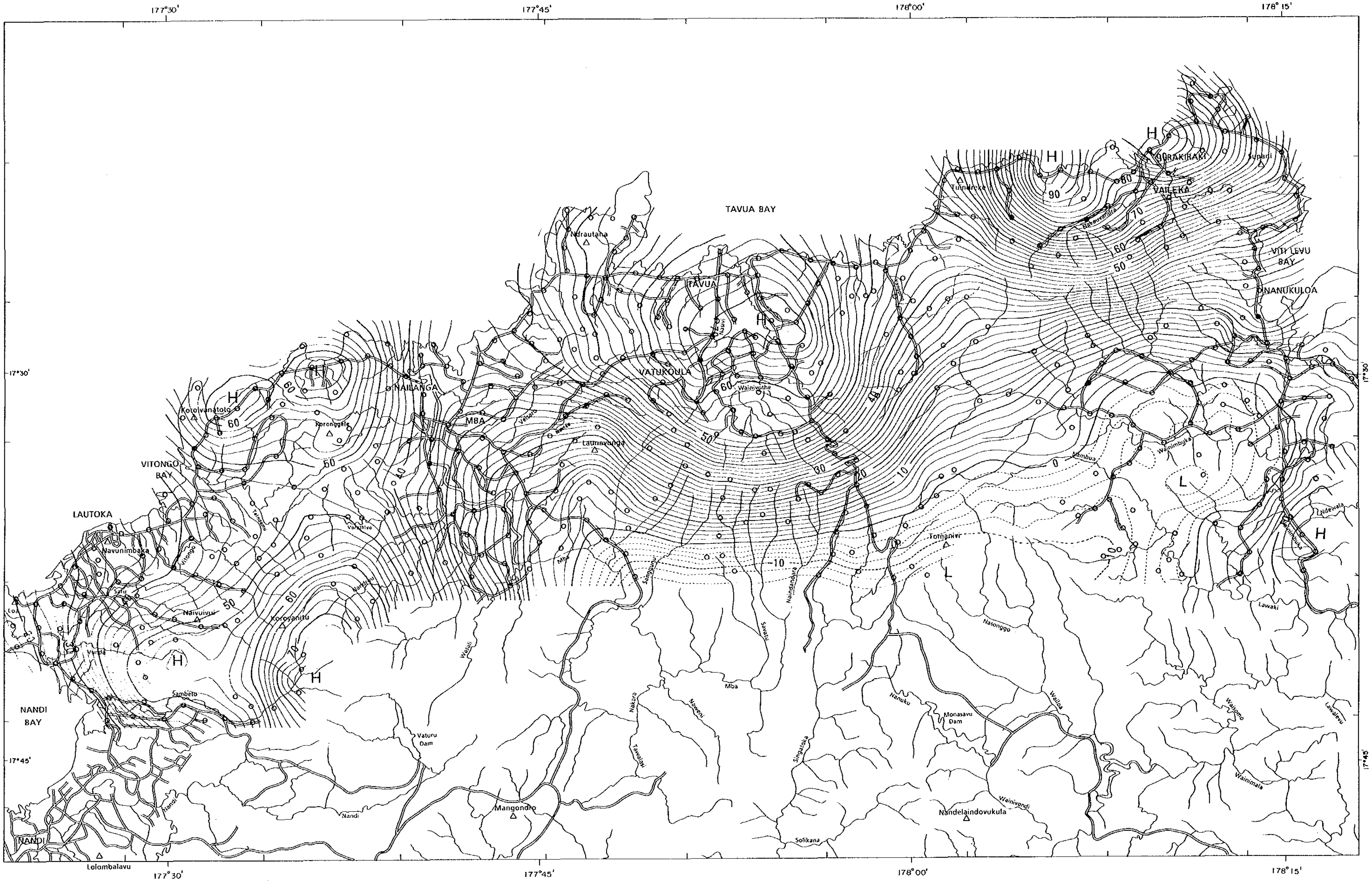

LEGEND

Contour interval : 2 mgal

SCALE 1:250,000

0 5 10 15km

Fig. 2-3-7 Bouguer Anomaly Map
(ρ = 2.5 g/cm³)

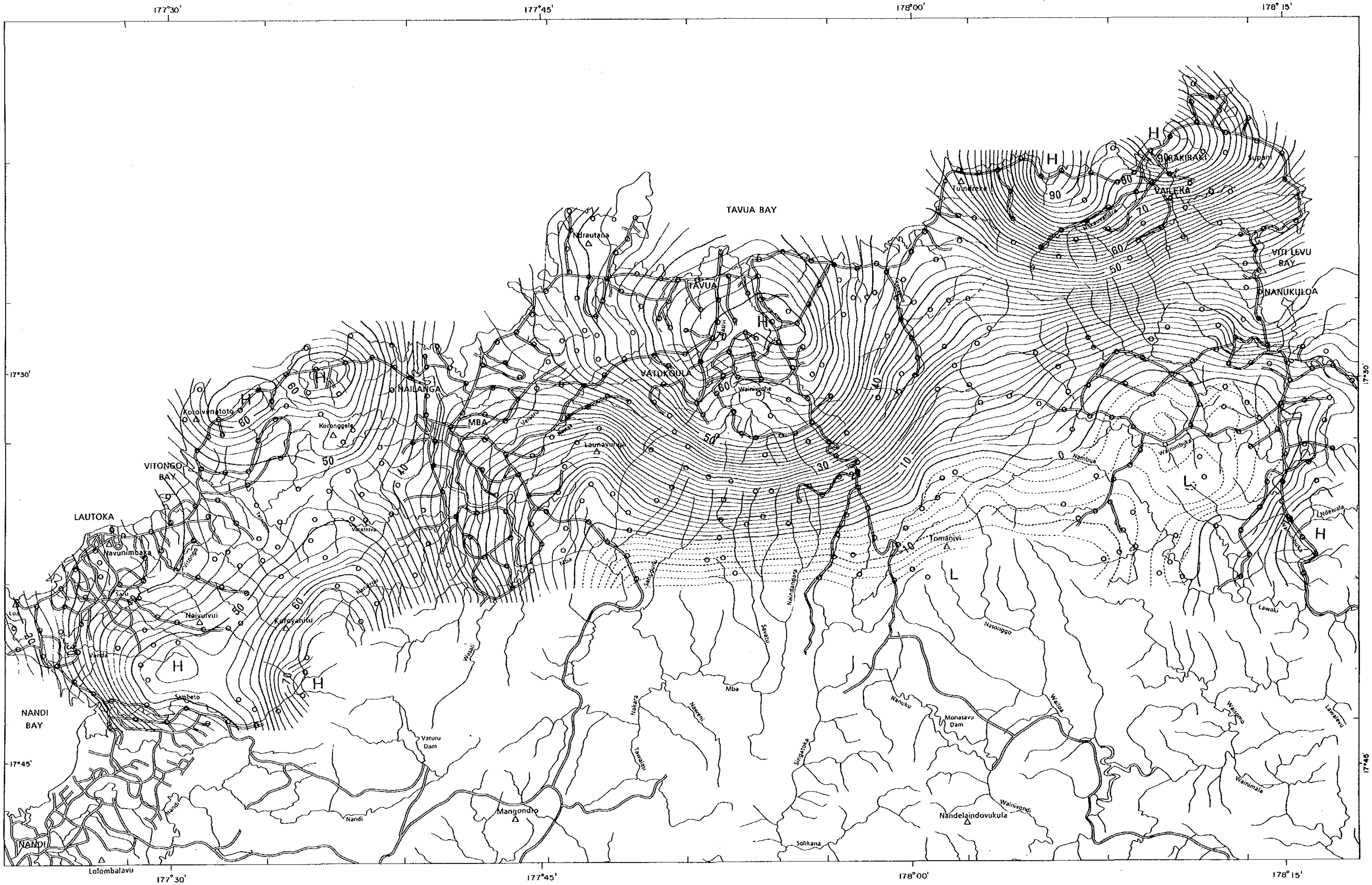

LEGEND

Contour interval : 2 mgal

SCALE 1:250,000

0 5 10 15km

Fig. 2-3-8 Bouguer Anomaly Map
(ρ = 2.6 g/cm³)

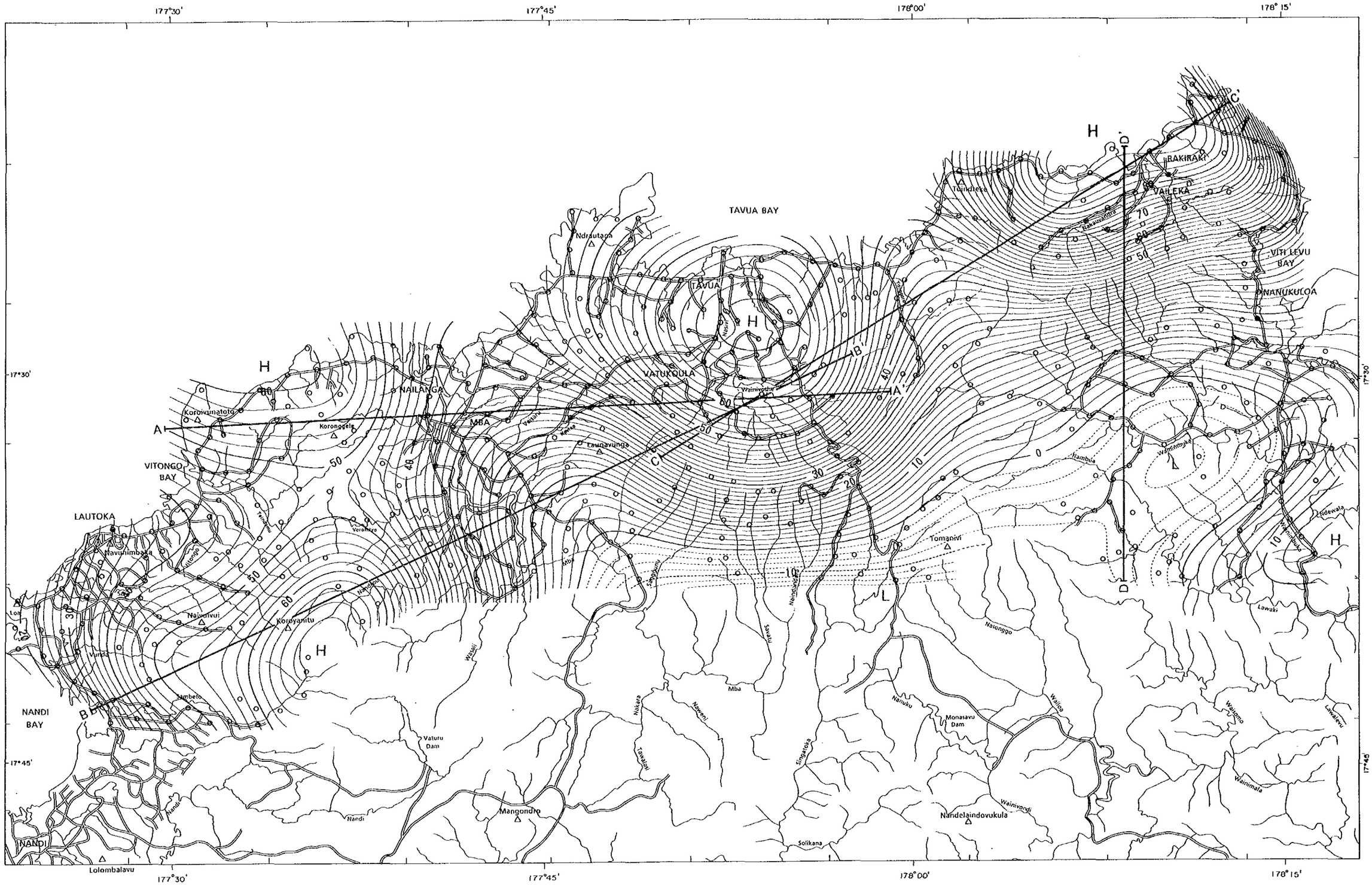

LEGEND

Contour interval : 2 mgal

A-A' Section line

SCALE 1:250,000

0 5 10 15km

Fig. 2-3-9 Long-wavelength Bouguer Anomaly Map

Figure 2-3-9. It is seen from Figure 2-3-7 and 9 that the contour intervals and shapes of both Bouguer anomaly map and long-wavelength gravity map are very similar except very minor details. This indicates that the Bouguer anomalies in this survey area is controlled mainly by the deep structures represented as long-wavelength anomalies.

(2) Short-wavelength gravity map

A short-wavelength gravity map with 1 mgal contour interval is shown in Figure 2-3-10. The contours are very sparse compared to those of the long-wavelength map.

The majority of the relatively large short-wavelength highs over 2 mgal are distributed within the gravity high zones (over 50 mgal) mentioned earlier. These zones are three localities west of Ba, three at Tavua Area, two at Rakiraki and two east of Nandi. Aside from these, relatively large short-wavelength gravity high was discovered near Nanukuloa at the eastern edge of the survey area.

Many of the short-wavelength gravity highs, with the exception of the two at east of Vatukoula, have circular to oval-shape. This shape is considered to indicate the existence of high density intrusive bodies in relatively shallow zones beneath the gravity highs.

The two short-wavelength gravity highs east of Vatukoula occur surrounding a short-wavelength gravity low of less than -2 mgal which have polygonal shape.

Low gravity anomalies almost totally disappear south of Nanukuloa where low density sedimentary formations are widely distributed and the gravity is around 0 mgal.

The short-wavelength gravity low elongated in the N-S direction southwest of Vatukoula is inferred to be caused by the shallow depth of the sedimentary rocks of the Nadi Group.

The short-wavelength gravity low southeast of Rakiraki is considered to be noise caused by filter analysis.

3-2-4 Profile analysis

Four-layered density structure is considered for this gravity survey

area. The four layers are, from the top downward; high density volcanic rocks, low density sedimentary rocks, high density igneous rocks and higher density rocks assumed to exist in the deeper zones.

In case of four-layered structure, it is generally difficult to obtain solution by analytical calculation alone. It is necessary to construct models based on information on subsurface geologic structures. In the case of the present gravity survey area, however, there are very few information regarding underground structure and analysis by density structure models was not feasible.

Therefore, profile analysis was applied for the study of this area. Short- and long-wavelength gravity anomalies were used for the analysis as follows. Short-wavelength gravity was used for the shallow zones, designating the high-density volcanic rocks as the first layer and the low-density sedimentary formations as the second layer. And long-wavelength gravity was used for the deeper zones, designating the units down to Yavuna Group as the first layer and the deeper assumed high-density rocks (amphibolite, granulite) as the second layer.

When gravity anomaly in the shallow zone occurs widely and extensively, this could be interpreted as cause by deeper seated structure and extracted as long-wavelength anomaly. In such a case the solution from the profile analysis using short-wavelength anomalies will be qualitative. Also for analyses of deep structures using long-wavelength gravity, the solution becomes phantom solution because of the lack of data on the second layer.

In the analysis for shallow structures, two cases were considered, one with the density difference between the first igneous layer and the second sedimentary layer to be 0.5 g/cm^3 and the other 0.3 g/cm^3. For deep structure analysis, the density of the first layer was assumed to range from 2.5 to 2.7 g/cm^3 and that of the second layer from 3.0 to 3.2 g/cm^3 with density difference of 0.5 g/cm^3 and calculations were made with two different control point depths.

As shown in Figures 2-3-9 and 10, four analysis profiles were constructed to pass through the gravity highs of the four zones(Fig.2-3-11 to 14).

Regarding the control points, the surface near the center of the igneous-sedimentary boundary, the B-B′ section was set for shallow structure

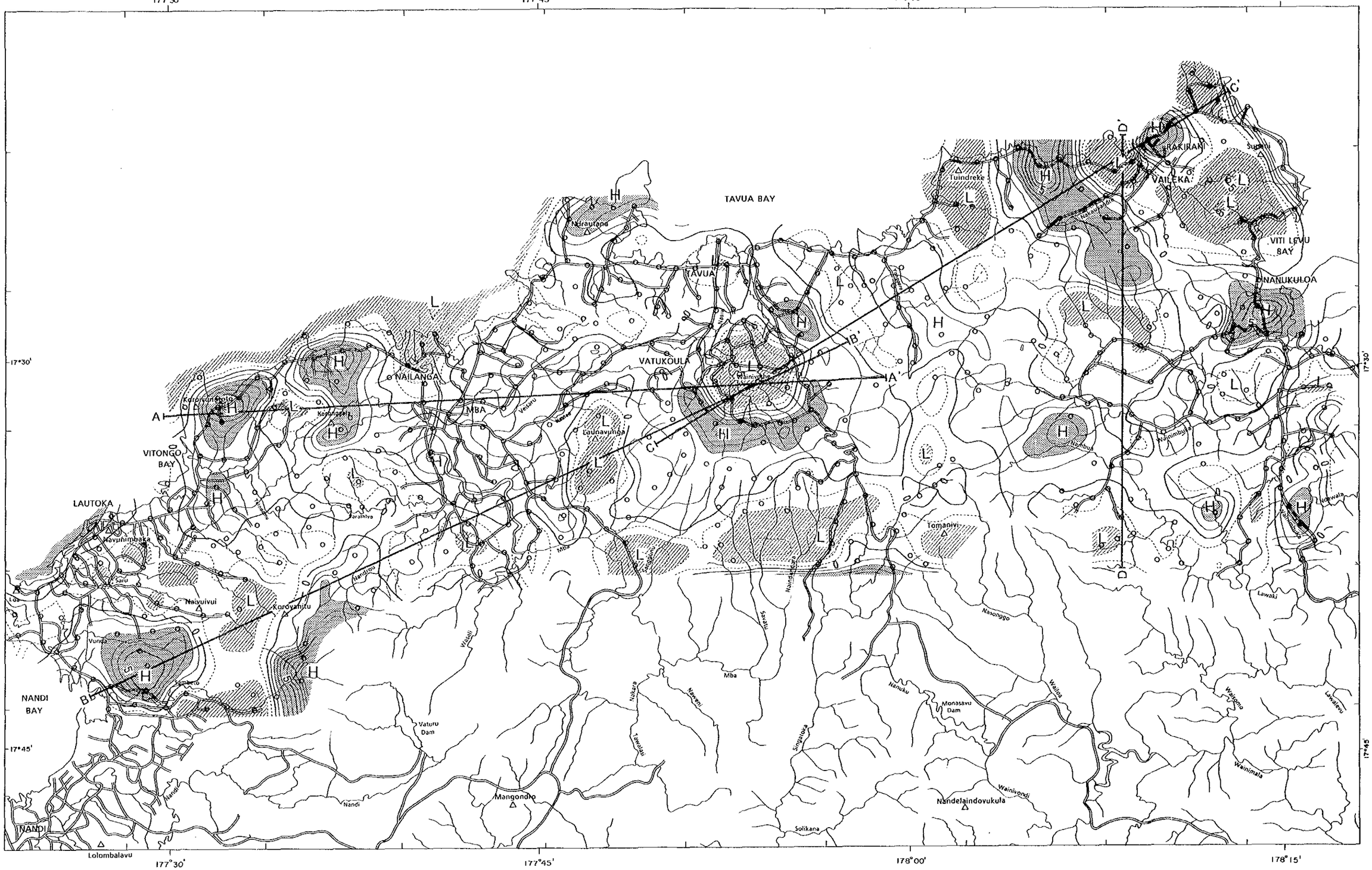

LEGEND

Contour interval : 1 mgal

A-A' Section line

Gravity high (>2mgal)

Gravity low (<-2mgal)

SCALE 1:250,000

0 5 10 15km

Fig. 2-3-10 Short-wavelength Bouguer Anomaly Map

analysis, and the boundary depth was assumed to be 5 km and 8 km at the northern end of D-D' section for deep structure analysis.

In the shallow profile analysis using short-wavelength gravity anomalies shown in Figures 2-3-11 to 14, the depth of the upper surface of the second layer varies in a narrow zone between the surface and 1 km depth. This is considered to be caused by the extraction of the wide spread shallow anomalies as long-wavelength gravity anomalies caused by deep structures.

In the deep profile analysis using long-wavelength gravity anomalies, the above depth varies between 5 and 15 km when the control point was set at 5 km depth and between 8 and 25 km when set at 8 km. These figures show that calculated values do not agree with observed values and a model with more relief must be constructed.

3-3 Discussions

The gravity interpretation map shown in Figure 2-3-15 includes plots of; high and low gravity anomalies, short-wavelength high and low gravity anomalies, gravity lineaments, SLAR annular and dome structures, alteration zones, mineral prospects, high magnetic anomalies and the distribution of sedimentary rocks. The results of the gravity survey are considered as follows from this map.

High gravity anomalies exceeding 50 mgal were detected at four zones, namely west of Ba, Tavua, Rakiraki and east of Nandi. These gravity highs are considered from the size and shape to be caused by deep structures(over 5 km). Thus in these zones, high density rocks such as metamorphics are inferred to occur in zones shallower than other parts of the gravity survey area.

The majority of the short-wavelength gravity highs (over 2 mgal) are distributed in the above four zones. Relatively large short-wavelength gravity high was found near Nanukuloa which is not in the high gravity zone. These short-wavelength gravity highs are considered from their size and shape to have been caused by relatively shallow(1-3 km depth) high density rocks.

The short-wavelength gravity highs east of Vatukoula are an exception to the above. These anomalies are distributed surrounding a short-wavelength

gravity low (under -2 mgal) and a collapsed structure associated with a polygonal fault structure is inferred regarding these anomalies. These collapsed structures are inferred to exist, although not very clearly, at west of Ba and at Rakiraki Area.

The annular and dome structures are clearly extracted by SLAR analysis in the four gravity high zones. These annular and dome structures correspond very well with the short-wavelength gravity highs. Three highs agree well with the structures west of Ba, two at Tavua, one at Rakiraki and two east of Nandi.

Many of the alteration zones occur within the short-wavelength gravity highs or in the vicinity. At east of Vatukoula, many alteration zones are distributed along the gravity lineaments. The relatively large alteration zones south of Ba are located out of the gravity survey area and its relation to gravity anomalies is not clear.

The mineral prospects, with the exception of that west of Ba, occur in the short-wavelength gravity highs or the vicinity. The Emperor Mine is located over the gravity lineament.

Magnetic highs and short-wavelength gravity highs agree well east of Nandi, but, on the whole, they do not correlate very well. This is considered to be caused by the magnetic anomalies reflecting the magnetism of the surface rocks while the short-wavelength gravity highs reflect the subsurface intrusive bodies.

The gravity high zones and short-wavelength gravity highs agree very well with the SLAR annular and dome structures, the alteration zones and the mineral prospects. In order to clarify the detailed correlation of these data, however, gravity survey with closer station interval is necessary.

The overall form of the gravity high east of Nandi is not clear because of its location at the southern end of the gravity survey area. There are many alteration zones and prospects in this zone and survey in the south of the present area is desired.

The gravity highs at east of Nandi, Tavua and Rakiraki occur on an ENE-WSW line at almost equal interval. This direction is that of the deep fracture zone of Viti Levu and the possibility of encountering such gravity highs in the southern extension of this line is considered.

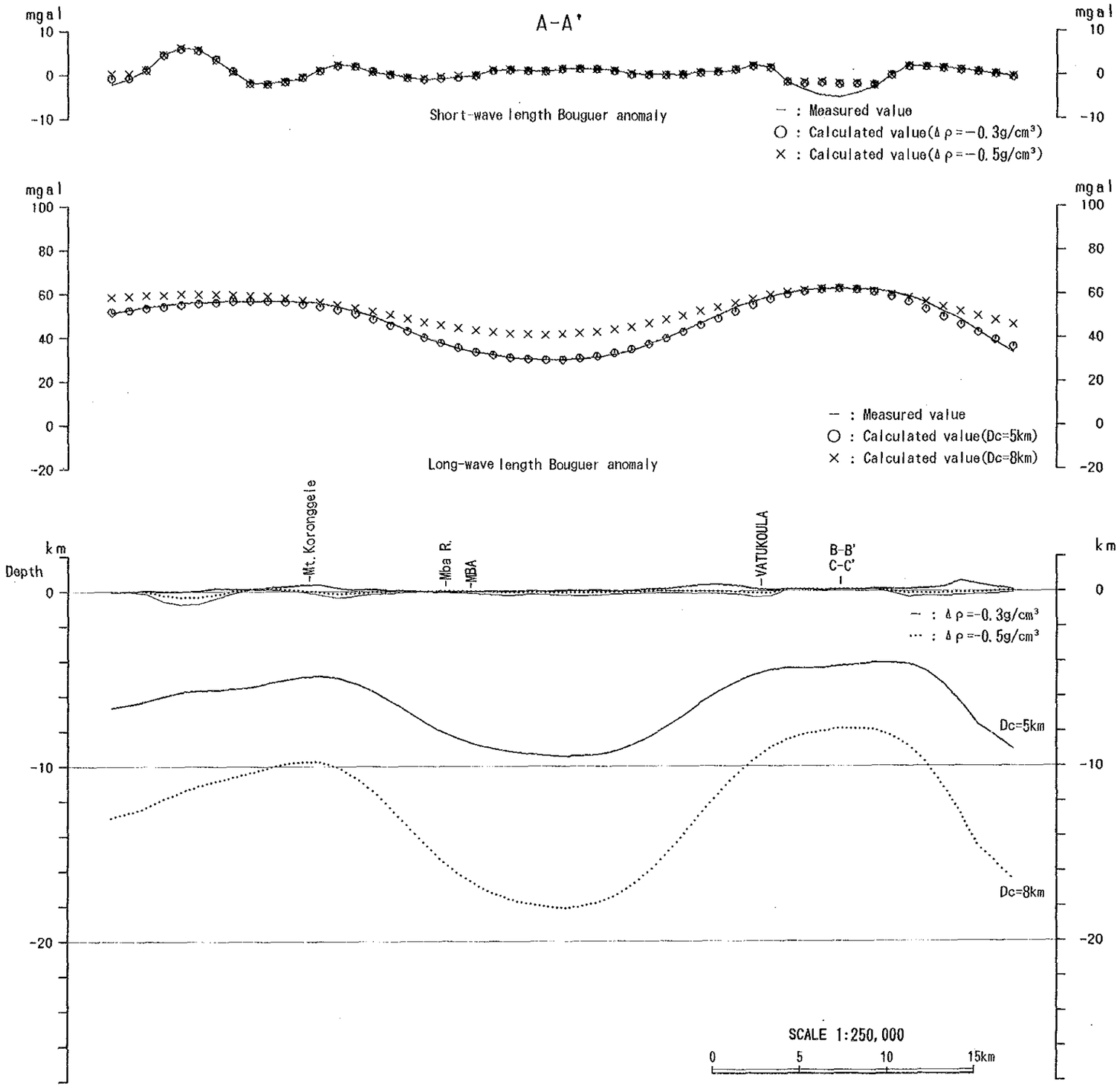

Fig. 2-3-11 Gravity Analysis Profile A-A'

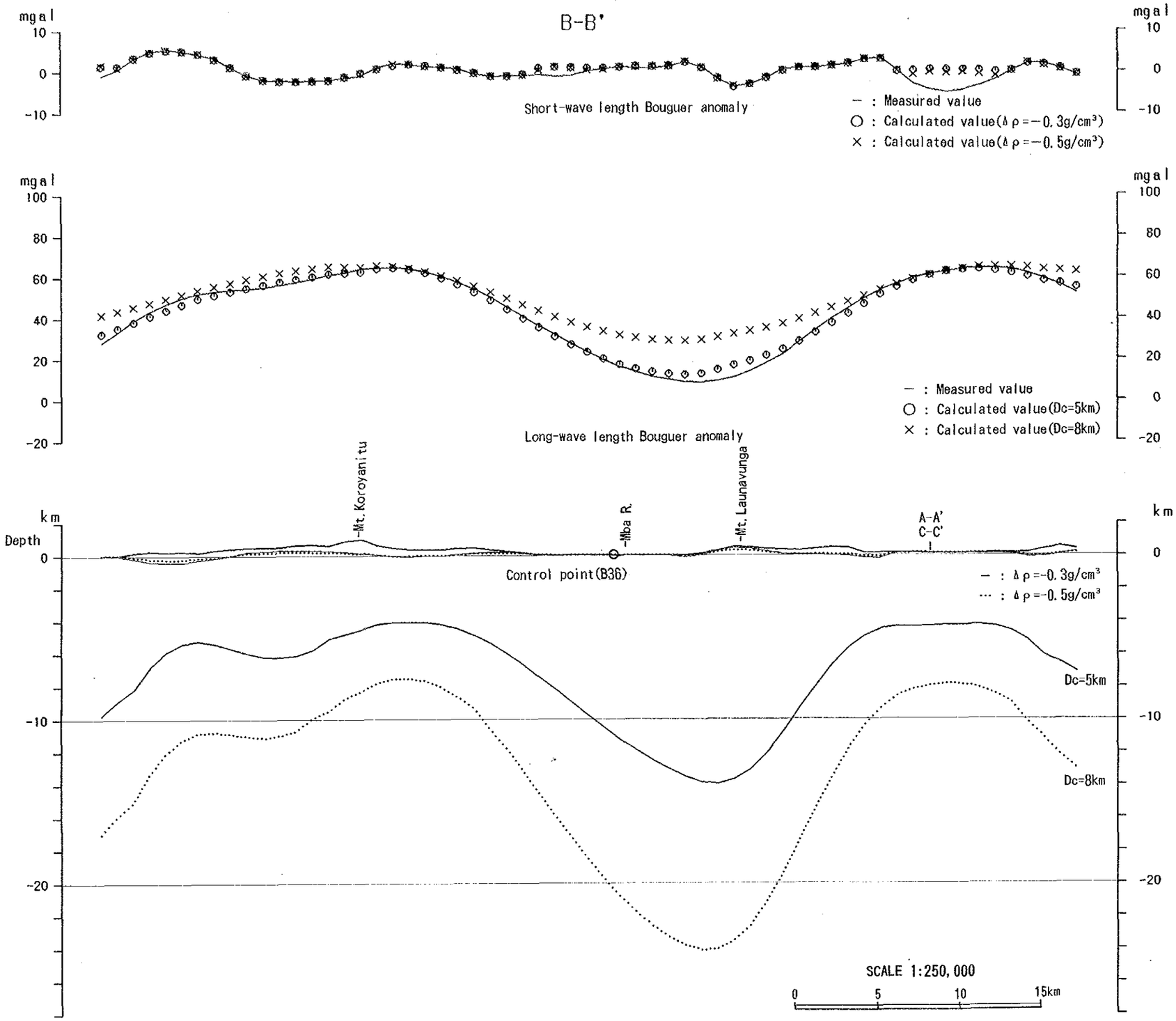

Fig. 2-3-12 Gravity Analysis Profile B-B'

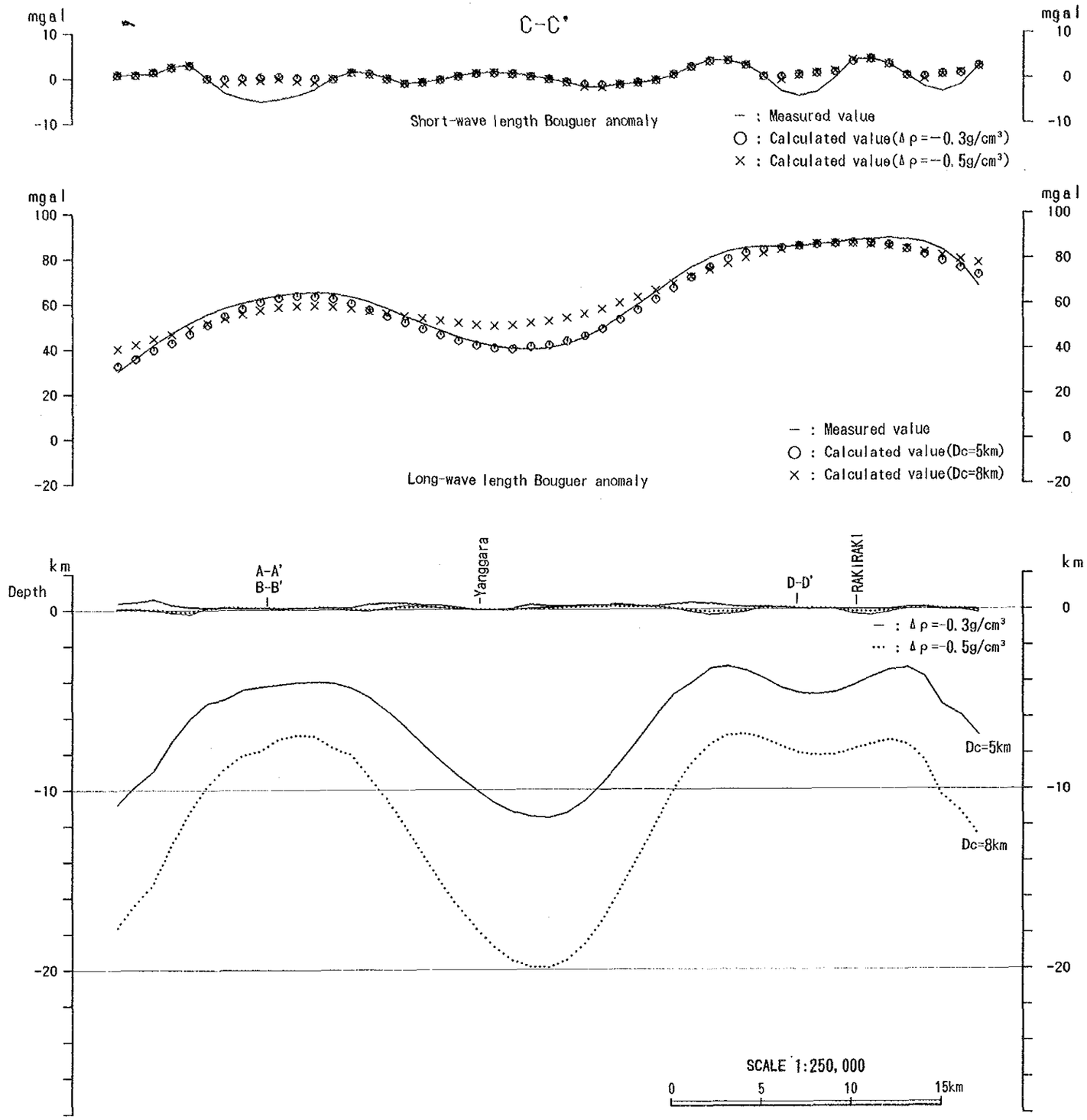

Fig. 2-3-13 Gravity Analysis Profile C-C'

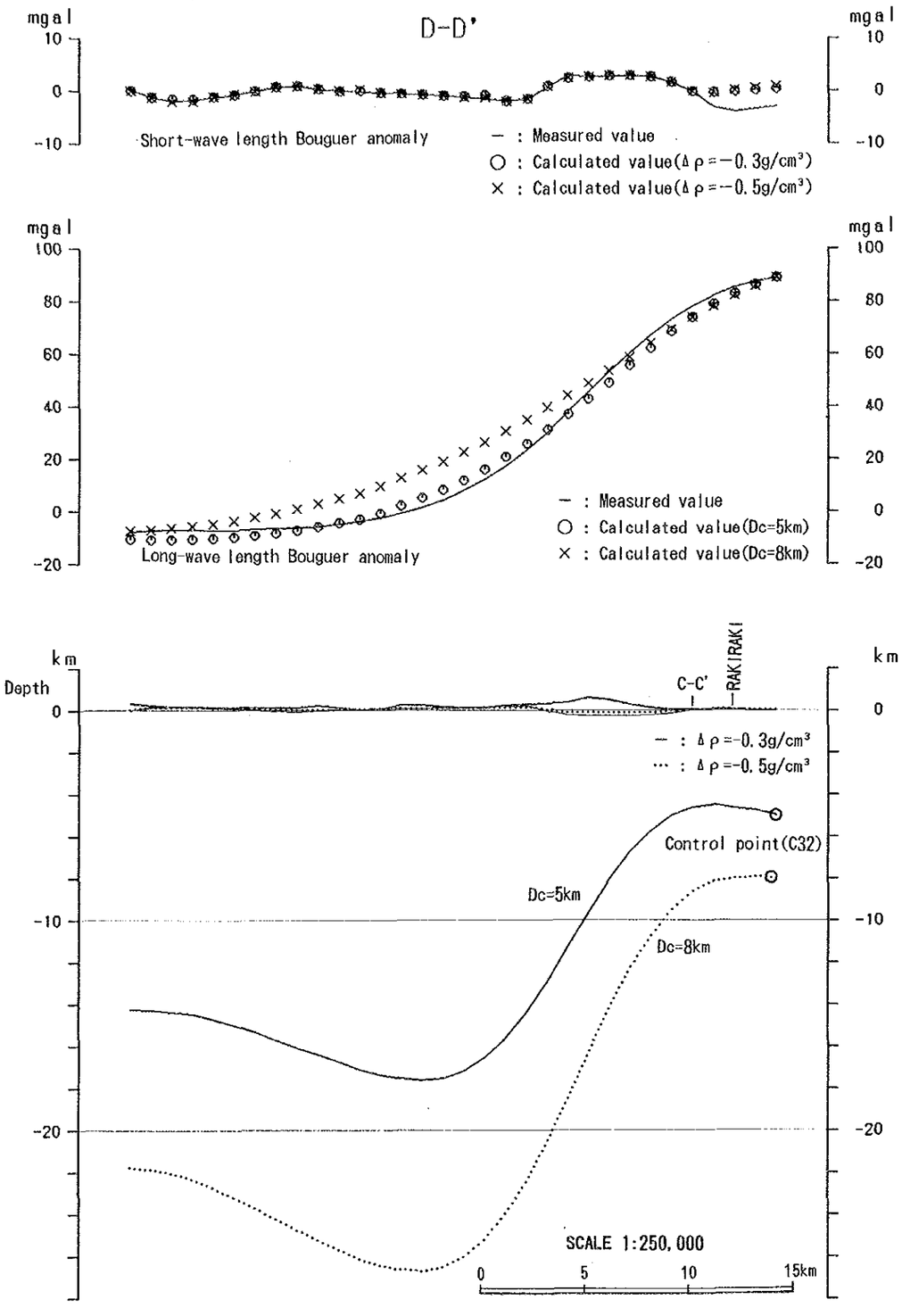

Fig. 2-3-14 Gravity Analysis Profile D-D'

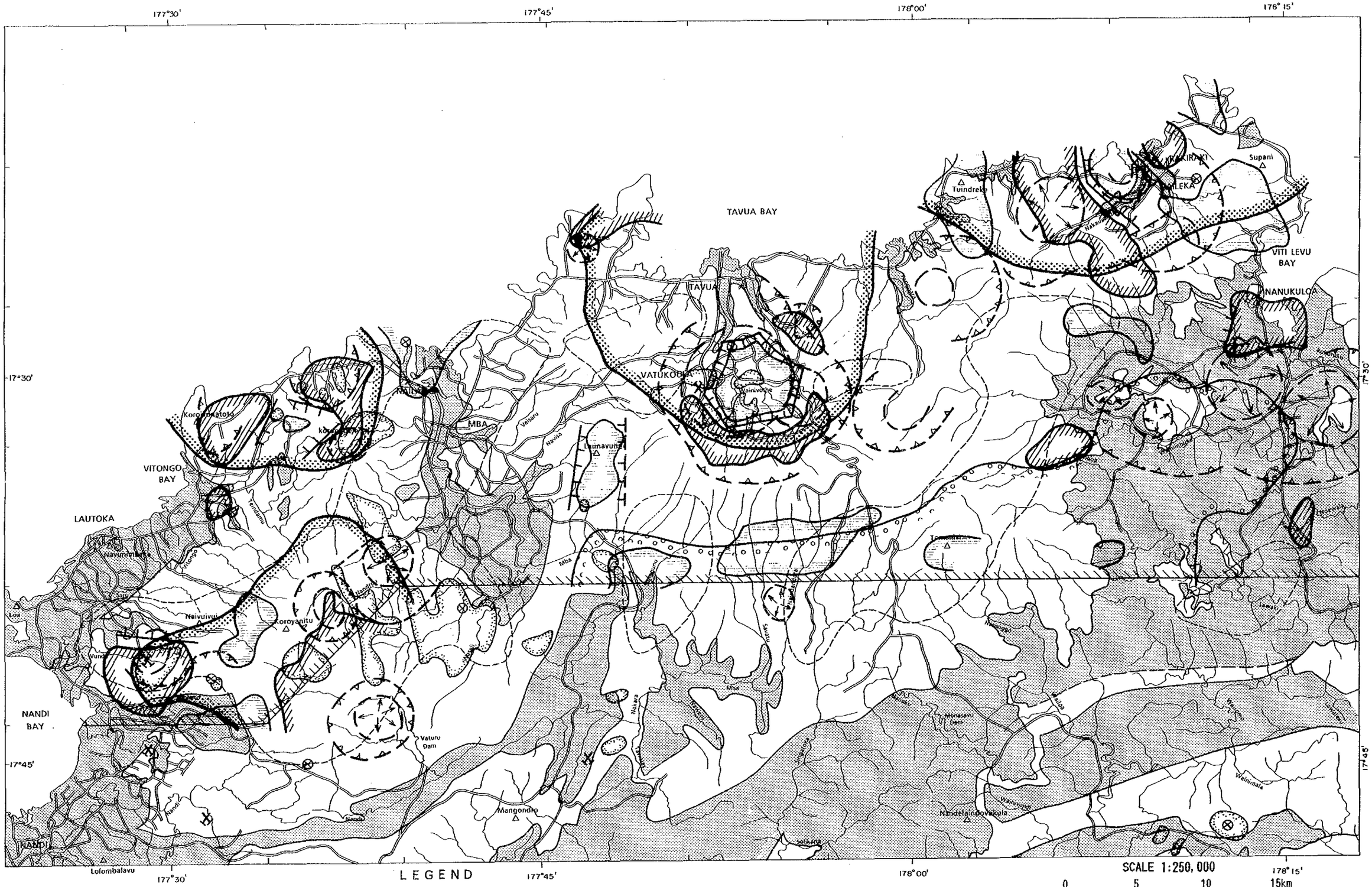

LEGEND

- Gravity survey area
- Gravity high zone(>50mgal)
- Gravity low zone(<0mgal)
- Short-wavelength gravity high(>2mgal)
- Short-wavelength gravity low(<-2mgal)
- Gravimetric lineament
- Annular structure on SLAR
- Caldera structure on SLAR
- Dome structure on SLAR
- Magnetic high anomaly(>500gamma)
- Alteration
- Sedimentary rocks
- Working mine
- Closed mine
- Prospect

Fig. 2-3-15 Gravity Interpretation Map

PART Ⅲ CONCLUSIONS AND RECOMMENDATIONS

PART III Conclusions and Recommendations

Chapter 1 Conclusions

During the course of the first phase of the Viti Levu Island survey, compilation of all existing geoscientific data and information of Viti Levu (area of 10,400 km^2), analysis and interpretation of SLAR imageries and SPOT images, field geological survey, and gravity survey (517 stations) of Tavua area (2,000 km^2) in the northern part of the island were carried out with the following conclusions.

(1) Twelve geologic units were delineated by SLAR imagery interpretation and 13 units by SPOT interpretation.

(2) Anticlinal and synclinal structures extracted from SLAR imageries and SPOT images are distributed from the central to the southern part of the island.

(3) A total of 1,060 lineaments were extracted from SLAR imageries. Many of these lineaments are considered to have been formed associated with the lateral faults caused by maximum horizontal compressional stress in three main directions. Most of the mines and mineral prospects of Viti Levu, with the exception of bedded manganese, residual, placer deposits and those of the western part, occur within the zone of lineaments formed by ENE to ESE trending horizontal stress or in the vicinity.

(4) It was seen from SLAR studies, that annular structures and caldera structures occur in the vicinity of the epithermal gold deposits of the Emperor Mine, and that annular, caldera and dome structures exist near the Namosi porphyry copper deposit. These photogeologic structures were interpreted to reflect the intrusion of magma in the area. Working on this hypothesis, 15 areas which contain at least one of the SLAR annular, SLAR caldera and SLAR dome structures were selected. From these 15 areas, Rakiraki, east of Vatukoula, upper reaches of the Mba River, northeast of Nandi and South of Mba area were selected as having strong geoscientific semblance to the area near the Emperor Mine. Also northeast of Nandi and South of Mba area were selected as areas with geologic environment very similar to the Namosi Deposit area.

(5) The geology of Viti Levu consists mainly of Late Eocene-Early Oligocene

volcanic and plutonic rocks, Late Oligocene-Middle Miocene volcanic and sedimentary rocks, Middle to Late Miocene plutonic rocks, Late Miocene-Early Pleistocene volcanic, plutonic and sedimentary rocks, and Pleistocene-Holocene sediments.

(6) Large number of faults occur to the south of the Colo Plutonic Suite in the central part and near the Yavuna Group in the southwest. ENE and NW trending faults are predominant to the south of the Colo Plutonic Suite while those with ENE to NNE and NNW trend are developed in the Colo Plutonic Suite zone. Faults with various trends occur in the vicinity of the Yavuna Group.

(7) A large number of folds occur in zones of many faults. Anticlines and synclines occur parallel to the elongation of the plutonic rocks (ENE to ESE, NNE) near the Colo Plutonic Suite zone and anticlines and synclines of many trends occur in the Yavuna Group zone in the southwest.

(8) The direction of the maximum horizontal compressional stress inferred from the lineament analysis and the distribution of the Colo Plutonic Suite is ENE to ESE during Late Miocene and after Middle Pliocene, NNW to NNE during latest Miocene-Early Pliocene, NW during Early-Middle Pliocene. It is inferred, thus, that compressional stress in the ENE to ESE direction affected the area for the longest period in geologic history resulting in the largest number of basins elongated in this direction and of deep fissures also with this trend.

(9) The locations of the centres of the volcanism of the latest Miocene - earliest Late Pliocene Ba Volcanic Group were inferred from the distribution of the volcanic rocks and the photogeologic annular, caldera and dome structures. It is considered from the above that volcanic chains existed extending in the ENE direction in northern Viti Levu and in the NW direction in the eastern part of the island. These volcanoes are believed to have formed over the deep fissure zones.

(10) Many of the lineaments formed under latest Miocene-Early Pliocene NNW to NNE compressional field are distributed in the west and northwest to southeast Viti Levu. On the other hand, NW trending deep fissures are believed to have existed from northwest to southeast Viti Levu at that time. This is inferred from the distribution of the then active volcanic rocks, locations of the volcanic centres at the time and the distribution of the

above lineaments.

(11) Large scale high gravity anomalies were discovered in four localities at west of Mba, Tavua caldera, Rakiraki and east of Nandi. It is inferred that these anomalies reflect the fact that high density rocks (amphibolite, granulite and others) occur at shallower depths at the four localities than in the surrounding areas.

(12) The zones where volcanic centres are inferred to have existed in northern Viti Levu correspond to the zones of short-wavelength high gravity anomalies related to basaltic activities. It is believed that since the contents of the magmatic chambers of that time has changed from basalt to olivin-gabbro of higher density, there are positive gravity anomalies near the altered volcanic centres. However, even in cases of Kilauea type caldera, the interior of the caldera is filled with thick, compact lava which is more dense than the whole volcano and thus the centre of eruption would show somewhat higher density.

(13) The Tavua Caldera whose upper parts are filled by low density formations such as andesitic pyroclastics and lacustrine sediments show short-wavelength low gravity anomaly surrounded by gravity lineaments. The SLAR annular structure zone near Rakiraki in northeast Viti Levu and the vicinity of the volcanic centres west of Mba are the zones which have Tavua Caldera type gravity structure among the possible collapse caldera zones extracted photogeologically.

(14) There are distinct differences in the magnetic anomalies of the north and south Viti Levu. The anomalies in the north have very large amplitude with small size and consequently it is believed to have been caused by strongly magnetic bodies at shallow depth. The surface is widely covered by Ba Volcanic Group and the individual magnetic anomalies could be reflecting the lithological variation in this Group.

Whereas in the south, large scale magnetic anomalies occur. The Colo Plutonic Suite and the Yavuna Group zones correspond to the magnetic high zone (over 500 γ) while the distribution of Wainimala and Medrausucu Groups correspond to the low magnetic anomalous zones with fair degree of agreement.

It is possible that Colo Plutonic Suite exist in deeper zones at the

large high magnetic anomalous zone in the eastern part. Also the Yavuna Group or intrusive bodies may exist in the large magnetic high in the northwest.

(15) Vein, network dissemination, porphyry copper, replacement, skarn and sedimentary type mineralization occur in this survey area.

The vein and dissemination types are grouped into epithermal gold and meso-hypothermal base-metal mineralization. The epithermal group is further classified into adularia-sericite type and acidic sulfate type. The epithermal gold mineralized zones in the Ba and Koroimavua Volcanic Groups occur near the volcanic centres which were the source of the volcanic rocks or near the zones where these centres are inferred to have existed.

The epithermal gold mineralized zones are distributed in the ENE-WSW direction from the northern to western Viti Levu.

The porphyry copper type mineralization is classified into the plutonic and volcanic types.

The volcanic type porphyry copper mineralized zones occur within and the vicinity of the latest Miocene to Early Pliocene volcano-plutonic complex (Namosi Andesite of Medrausucu Group, Sabeto Volcanics · Navilawa Stock · Nawainiu Intrusive Complex of Koroimavua Volcanic Group).

The plutonic type porphyry copper and the meso to hypothermal base-metal mineralized zones occur within and the vicinity of the Middle to Late Miocene Colo Plutonic Suite.

The skarn type mineralization occurs in the contact zone of the Colo Plutonic Suite and Wainimala Group limestone. The replacement type mineralization occurs in the Wainimala Group in the vicinity of the Colo Plutonic Suite.

Sedimentary mineralization is divided into massive sulfide, bedded manganese, residual and placer type concentration.

The massive sulfide mineralization is stratabound type which occurs in pyroclastics of the Wainimala Group formed by submarine volcanic activity.

The major bedded manganese deposits are stratabound type which occur in the bedded volcano-sedimentary formations of the Wainimala Group. These also tend to occur near the replacement and skarn type mineralized zones.

The residual deposit found in Viti Levu is a small bauxite deposit formed by lateritic weathering of basaltic pyroclastics of the Ba Volcanic Group.

The placer deposits in the survey area are gold concentration in alluvium and iron oxides in deltas and sand dunes.

(16) The geologic environment necessary for the formation of epi-mesothermal deposits is the existence of magmatic heat, subsurface fractures and circulating water. The magmatic heat and the subsurface fractures are mostly likely to exist in volcanic collapsed and volcanic dome structures. The circulating water formed the mineralized and altered zones. Structures which are likely to be volcanic collapse and volcanic domes were extracted through photogeologic studies of annular, caldera and dome structures; short-wavelength gravity anomalies; and field survey. Of these zones; vicinity of Rakiraki, Tavua Caldera zone, area west of Mba to southern part, Sabeto Range south of Lautoka and Namosi area are considered to contain high potential for locating mineralized and altered zones.

Chapter 2 Recommendations for the Second Phase

(1) Geochemical prospecting and detailed geological survey

Of the areas extracted with anticipation of epithermal gold mineralization, that extending southward from west of Mba is relatively unexplored. This lies within a 20 km x 10 km area, extend in the NNW direction, alteration zones occur scattered inside, Balevuto Gold Prospect exists to the south, volcanic collapsed zones and volcanic domes probably exist to the southwest and north, and gravity structure similar to the Tavua Caldera exists in the northwest portion. From these features, the possibility of finding mineralization is considered to be high in this area. Promising mineral showings, however, have not been found yet. From the above reasons, geochemical prospecting and detailed geological survey for delineating promising zones in this area are recommended.

(2) Lineament analysis of aerial photographs

Close relationship between the distribution of mineralized zones and lineaments is inferred from the results of the SLAR imagery analysis. It is recommended that lineament analysis of aerial photographs be carried out and promising areas be delineated from the areas extracted as possessing high potential during the first year survey, namely vicinity of Rakiraki, Tavua Caldera, southward from west of Mba, Sabeto Range south of Lautoka, and the Namosi area.

(3) Gravity survey

In the western part of Viti Levu, the Yavuna Group which forms the basement of the island is distributed and the Colo Plutonic Suite intrudes into the Wainimala Group. Alteration zones occur widely in the NW to WNW direction around the Colo Plutonic Suite and porphyry and skarn type mineralized zones are distributed within these altered zones. Epithermal gold deposit (Faddy's) of acidic sulfate type occur in the Wainimala Group in the western edge of the island, but the factors controlling the mineralization are not clear.

It is considered from the above that western Viti Levu has a relatively high mineral potential. It is, thus, recommended that gravity survey be carried out in western Viti Levu and that the basement structure, subsurface distribution of Colo Plutonic Suite, the existence of volcanic centres be clarified by geological analysis. This will also clarify the high gravity anomaly zones and high magnetic anomaly zones and the relationship between

the geologic structure of the island and mineralization.

Epi-mesothermal mineralization occurs in the vicinity of the known and inferred volcanic centres. Also areas of these centres show gravimetric characteristics such as short-wavelength high gravity anomalies or short-wavelength low anomalies according to the difference of the nature of the volcanic activity. Thus, gravity survey is an extremely effective method for mineral exploration in this geologic environment and gravity survey of the entire Viti Levu with the exception of the area covered during the first year is recommended.